CR 86150

HIGH POWER L-BAND TRANSMITTER AND ULTRASTABLE OSCILLATOR FOR THE NAVSTAR SATELLITES

prepared for
Electronics Research Center
National Aeronautics and Space Administration

TRW
SYSTEMS GROUP

Mr. Peter Engels
Technical Monitor
NAS 12-539
Electronics Research Center
Cambridge, Massachusetts 02139

Request for copies of this report should be referred to:

NASA Scientific and Technical Information Facility
P.O. Box 33, College Park, Maryland 20740

NOTICE TO USERS

Portions of this document have been judged by the Clearinghouse to be of poor reproduction quality and not fully legible. However, in an effort to make as much information as possible available to the public, the Clearinghouse sells this document with the understanding that if the user is not satisfied, the document may be returned for refund.

If you return this document, please include this notice together with the IBM order card (label) to :

Clearinghouse
Attn: 152.12
Springfield, Va. 22151

08710-6021-R0-00

HIGH POWER L-BAND TRANSMITTER AND ULTRASTABLE OSCILLATOR FOR THE NAVSTAR SATELLITES

October 1968

Prepared Under Contract NAS 12-539 by

TRW Systems
One Space Park
Redondo Beach, California

ELECTRONICS RESEARCH CENTER
NATIONAL AERONAUTICS AND SPACE ADMINISTRATION

ACKNOWLEDGEMENT

The results of this report represent the efforts of Edmund Jurkiewicz of the Communications Laboratory and A.J. Mallinckrodt (Appendix C), consultant to TRW Systems Group.

A. Garabedian
Study Manager

CONTENTS

INTRODUCTION AND SUMMARY

This report discusses the two key items in the navigation signal subsystem of the NAVSTAR satellites, the L-band transmitter and ultra-stable oscillator or clock. The NAVSTAR interim report (Reference 1) proposed a 50-watt output solid-state design for the transmitter and a quartz crystal reference for the oscillator. This report discusses a refinement of that transmitter design along with two additional designs and a commercially available crystal oscillator which meets the NAVSTAR requirements and can be used for NAVSTAR satellite test programs.

Of the two additional transmitter designs, one is a straightforward approach using an L-band TWT power amplifier and the other incorporates a solid-state L-band power amplifier. This latter design promises to be the most attractive from all standpoints of design including reliability and DC-to-RF efficiency. Efficiency is expected to be greater than 30 percent. However, the design also contains an element of uncertainty since development depends on the availability of high-power integrated modules or chips. Work is now in progress on high power S-band modules at TRW Semiconductors. Present plans are that 20-watt modules will be developed in six to nine months; the design assumes the use of these modules scaled to operate at L-band.

The first solid-state design (basically the same as in the interim report) using state-of-the-art components is shown to be superior to a TWT design in all respects except DC-to-RF efficiency. An efficiency of 22 percent minimum is expected as compared to 28 percent minimum for the TWT.

A crystal oscillator is available from Frequency Electronics of New Hyde Park, N. Y., which has shown the capability to meet the stability requirements needed for the NAVSTAR system. Similar units have been flown in space and extensive data is available which support the stabilities claimed for the unit.

A test program is proposed which will verify the performance of the Frequency Electronics unit. In particular, a set of phase stability measurements are proposed from which variate difference statistics can be derived. These statistics demonstrate the expected time error in extrapolating oscillator drift as proposed in the NAVSTAR system.

The design of the L-band transmitter was investigated with the goals of maximizing DC-to-RF efficiency and reliability. Two solid-state designs and a TWT design were studied. The first solid-state design is based on existing components and circuit techniques. The key parameters of this design are compared to a TWT design. An S-band tube was assumed which can be easily scaled down to operate at L-band.

The second solid-state design is based on a projected solid-state power device which should be available in six to nine months. This projection is based on work being conducted at TRW Semiconductors. The basic difference between the two solid-state designs is the frequency at which the power amplification occurs. In the first approach, power amplification is at 500 MHz and a varactor diode tripler is used to increase the frequency to L-band. This approach is essentially the same as that proposed in Volume IV, Section 3.2 of Reference 1. In the second approach, power amplification is directly at L-band. This design has superior DC-to-RF efficiency because it avoids the loss in the varactor multiplier.

Table 1 lists the design parameters for the transmitters. A nominal carrier frequency of 1560 MHz is shown although the transmitter can operate anywhere in the 1540-1660 MHz band of interest. The 5 percent bandwidth specified is more than adequate to handle the signal modulation. The 50-watt output power is the minimum desired. Expansion to 100 watts is considered as growth potential.

The junction temperature of the transistors is restricted to 125°C maximum for reliability. This temperature is sufficiently degraded from maximum junction temperatures for silicon devices (200°C) to provide conservative design for reliability and is a generally accepted value for space application.

Not shown in Table 1 but nevertheless a requirement on the transmitter is the time division transmissions from the satellites. That is, the transmitter must be gated "on" and "off" with control signals. During

Table 1. Transmitter Design Parameters

Carrier frequency	1560 MHz
Bandwidth	5 percent or better
Power output	50 watts (growth to 100 watts)
Maximum junction temperature	125°C maximum
Baseplate temperature	50°C maximum
Input power from driver	1.6 watts at 520 MHz (design 1) 63 milliwatts at 1560 MHz (design 2) 50 milliwatts at 1560 MHz (TWT)
Input signal modulation	Phase modulation (PSK)
Input and output impedance	50 ohms
Overall DC-to-RF efficiency	Goal: 22 percent minimum (design 1) 31 percent minimum (design 2) 28 percent minimum (TWT)
Power supply	+28 V, ±2 percent
Input/output VSWR	1.5 maximum without breakup

"off" periods power must not be drawn from the power supply. This requirement is easily met by interrupting the signal input to the solid-state transmitter and the beam voltage on the TWT transmitter.

As a starting point in the design of the transmitter, an assessment must be made of the frequency at which power amplification should take place. The higher the frequency can be made the more efficient the transmitter should become because of the reduction in higher power level varactor multiplier stages. Amplification directly at L-band is preferred since high power varactor stages are eliminated.

The best available solid-state power device at the present time is the 2N5178 of TRW Semiconductors rated at 70 watts at 500 MHz at 25°C.

Presently available transistors that are capable of power gain at L-band have poor thermal resistance (θ_j). Consequently, the power output per transistor is limited to approximately 1 watt if the junction temperature is to be kept below 125°C. Therefore 50 transistors in parallel are required to produce 50 watts output.

Under development at TRW Semiconductors are integrated circuit S-band power modules developing 10 watts. It is projected that in approximately six to nine months 20 watts per module can be achieved.

2.1 SOLID-STATE WITH VARACTOR MULTIPLICATION

The first solid state design utilizes the 2N5178 power transistor operating at 520 MHz and the Varian LSP 811A-3 varactor diode as a tripler stage for increasing the frequency output to 1560 MHz. The available power output per transistor at 520 MHz is derived as follows. The thermal resistance θ_j of the transistor derived from the transistor specifications is

$$\theta_j = \frac{\text{maximum junction temperature - ambient temperature specified}}{\text{power rating}}$$

$$= \frac{200 - 25}{70} = 2.5^{\circ}\text{C/watt}$$

The maximum baseplate temperature is 50°C. An additional 10°C temperature gradient between the transistor case and baseplate is allowed, so that

$$\begin{aligned}\text{Device temperature rise} &= (\text{maximum allowable junction temperature}) \\ &\quad - (\text{maximum baseplate temperature}) \\ &\quad - (\text{allowable temperature gradient}) \\ &= 125 - 50 - 10 = 65^{\circ}\text{C}\end{aligned}$$

The total device dissipation is

$$P_d = \frac{\text{total temperature rise}}{\theta_j} = \frac{65}{2.5} = 26 \text{ watts}$$

The RF power output is given by

$$P_o = \frac{P_d}{\frac{1}{G} + \left(\frac{1 - \eta}{\eta}\right)} = 24.3 \text{ watts}$$

where

G = stage gain = 2.5 (4 db)

η = collector efficiency = 60 percent

Therefore, the total available output power per transistor at 520 MHz is 24.3 watts while maintaining the maximum junction temperature at 125°C with a baseplate temperature of 50°C and allowing an additional 10°C for the temperature gradient between the transistor case and the baseplate.

The efficiency of the times three multiplier is given by:

$$\eta = \left(\frac{n}{\gamma}\right)^2$$

$$\text{and } \gamma = \left[M + \sqrt{M^2 + 1}\right] \times n$$

where n = harmonic number

$$M = \frac{\pi}{2} \left(\frac{n^2 - 1}{n}\right) \times \frac{f_o}{f_c}$$

The best available varactor diode, the Varian LSP 811A-3, has f_c = 90 GHz. Therefore, M = 0.07 for

f_o = 1560 MHz

f_c = 90 GHz

n = 3

and the efficiency η is 86 percent for a loss of 0.7 db. The overall efficiency of the x3 multiplier, including the input, output and idler circuits, is assumed to be 63 percent, equivalent to a 2 db loss in the multiplier.

The diode thermal resistivity is given as 4.7°C per watt. Hence, maximum power dissipation per diode is

$$\frac{\text{maximum allowable temperature rise}}{\text{thermal resistance}} = \frac{65}{4.7} = 13.8 \text{ watts}$$

The minimum number of transistors and varactor diodes required for the transmitter are calculated below.

	50-watt Output	100-watt Output
Input power to x3 multiplier	$\frac{50}{0.63} = 80$ watts	$\frac{100}{0.63} = 159$ watts
Number of diodes	$\frac{(1 - 0.86)(80)}{13.8} = 0.8$	$\frac{(1 - 0.86)(159)}{13.8} = 1.6$
Number of transistors	$\frac{80}{24.3} = 3.3$	$\frac{159}{24.3} = 6.6$

With the aid of the preceding analysis, the following design approach was selected:

1) 50 watts at 1560 MHz will be obtained by combining the output power from two identical paths, each delivering 40 watts minimum at 520 MHz. The 40-watt outputs will be derived from three transistors in parallel. Two transistors would suffice; three are used for a conservative design and to keep the junction temperature below 125°C for increased reliability.

2) A x3 multiplier containing two varactor diodes in each path delivers 25 watts minimum at 1560 MHz to the combiner. A balanced configuration is used in the multiplier to reduce odd harmonics. Combining the two outputs at 520 MHz and then multiplying was rejected because of increased design problems with the multiplier at the higher power levels.

3) Growth to 100 watts at 1560 MHz is possible by using four or five transistors in parallel in each path delivering 80 watts minimum at 520 MHz. This power level is not recommended because paralleling more transistors increases balancing problems in combining the outputs. Thermal design and arcing at the output become more severe problems especially under the constraints of packaging size and weight.

Figure 1 shows a simplified block diagram of the entire transmitter. The driver and phase modulator are straightforward. The driver delivers 1.6 watts at 520 MHz to the solid-state power amplifier. The DC power input to the modulator and driver will be approximately five watts. Figure 2 is a detailed block diagram of the power amplifier showing the gain and power levels at each stage. This design uses a minimum number of active stages.

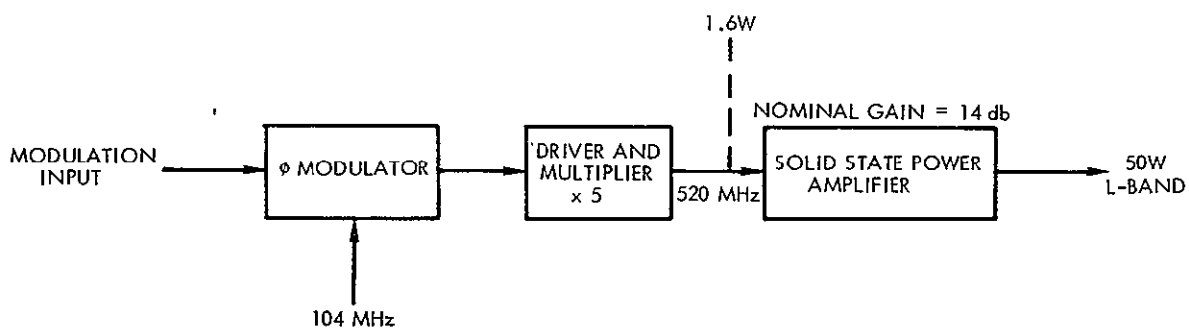

Figure 1. Simplified Block Diagram of Transmitter

The phase-modulated 520 MHz carrier from the driver is applied to the input stage A1, which is a single stage Class C amplifier exhibiting approximately 5 db of gain. The output feeds a 3 db power divider which, in turn, excites two identical transistor chains. A2, similar to A1, raises the power level to approximately 8 watts. The power divider that follows excites a Class C doublet amplifier, the output of which is combined in the hybrid to produce over 18 watts. This, in turn, provides an input to a 1:3 power divider feeding the Class C triplet. The combined outputs in the hybrid that follows yields over 40 watts. The basic circuit for each transistor stage is shown in Figure 3.

The x3 unit utilizes two varactor diodes in a balanced configuration. The two multiplier outputs at 27.5 watts and 1560 MHz are then combined to produce 54 watts at L-band. The unwanted outputs are 20 db down at this point, but if greater suppression is required, a bandpass filter (three-pole will produce approximately 36 db of suppression with a bassband loss of 0.3 db) can be added after the output combining network.

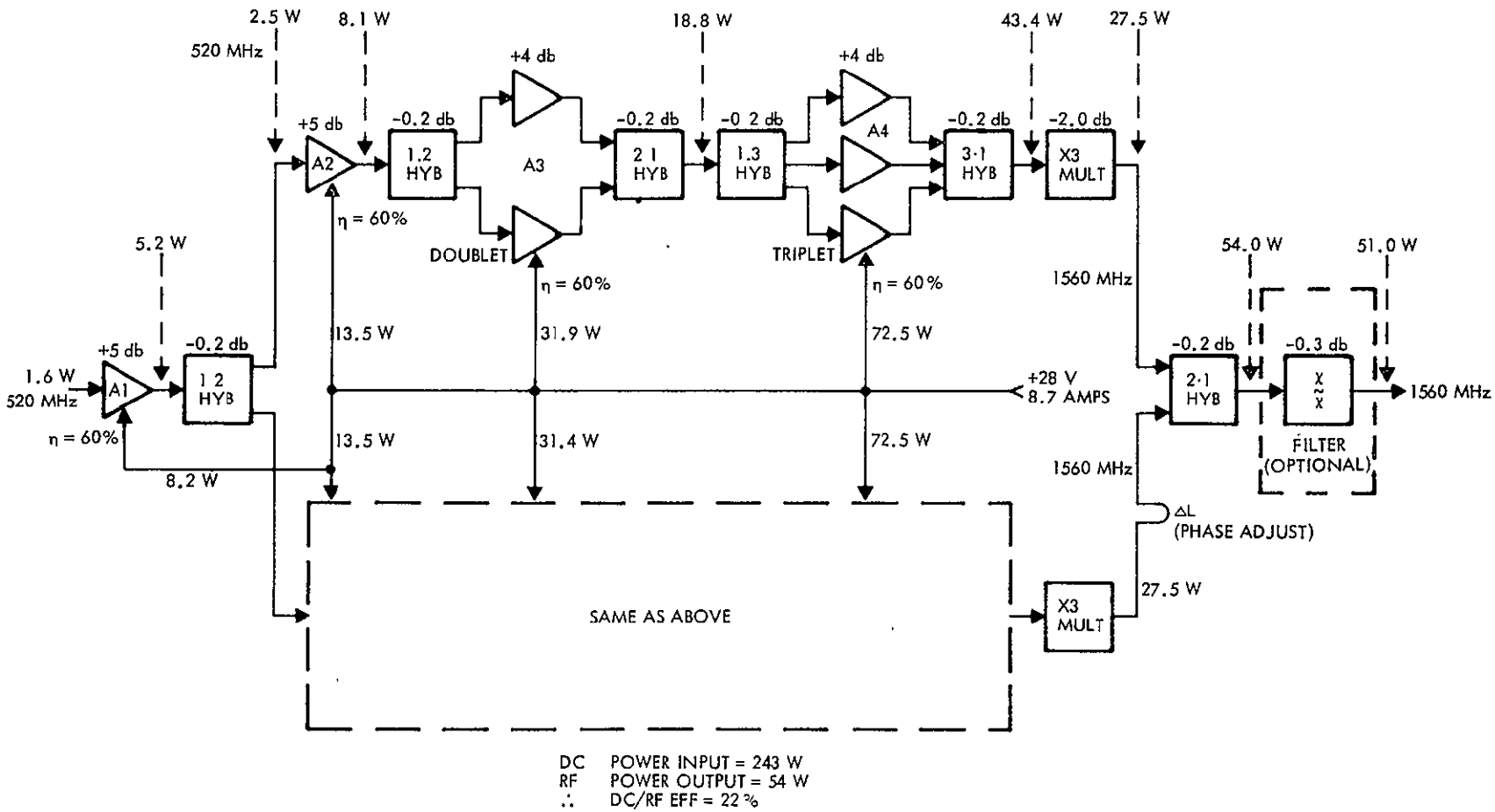

Figure 2. Block Diagram, Power Amplifier

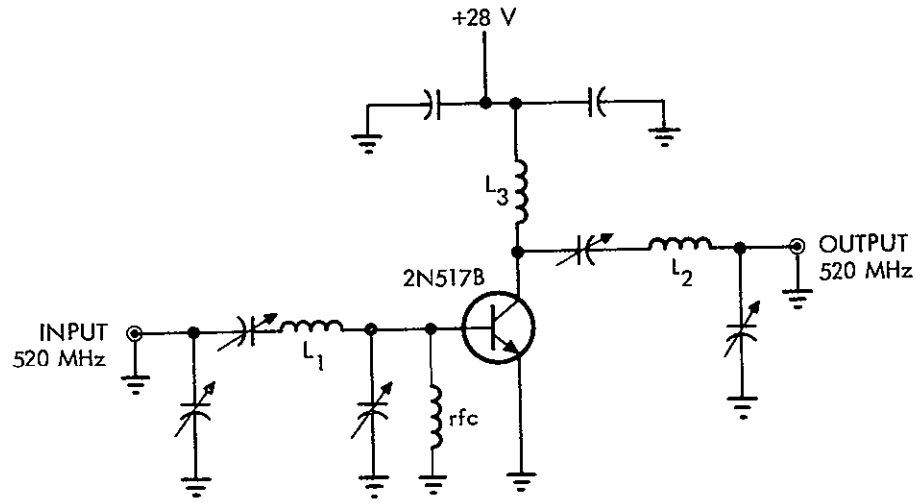

Figure 3. Basic Transistor Stage

The total number and types of transistors and varactor diodes required are as follows:

Stage	Number	Type
A1	1	PT 6680
A2	1 x 2	2N 5177
A3	2 x 2	2N 5177
A4	3 x 2	2N 5178
	13	Total transistors
x3	2 x 2	LSP 811A-3
	4	Total varactor diodes

The overall DC-to-RF efficiency of the transmitter is estimated to be not less than 22 percent; depending upon the availability of efficient high frequency varactor diodes, the design goal is 25 percent. The transmitter requires a +28 volt regulated (2 percent) power supply. Excluding output filter, the transmitter is estimated to weigh 4.5 pounds maximum and can be packaged in 12" x 5" x 2" or 120 in^3.

The following are the critical design areas for the transmitter.

1) A typical power combining network is shown in Figure 4. This technique allows a summation of "n" ports. The design is quite simple, yet care must be taken to insure identical path lengths for each input leg. To validate this design a power triplet (Figure 1, Stage A4) has been designed, built (Figure 5) and tested to deliver 50 watts at 500 MHz. The transistors used were prototype units of the 2N5178. Test results are given in Table 2. In Figure 5 quarter wavelength coaxial transmission lines are coiled in order to save space. The main feature of this design is that transistors operating in parallel are isolated from each other by a hybrid.

2) The x3 multiplier requires particular attention in order to find the optimum varactor diode to maximize the efficiency. The losses in the input, output, and idler circuits must also be minimized. The design is based on a 50-ohm input/output impedance so that the unit can be aligned and tested independently of the entire transmitter, diminishing the interface problems.

3) Another area that will require particular attention is the final power combiner. The correct summation of the two multiplier outputs depends upon phase coherency of the signals. Final phase adjustment on one of the combiner inputs will be necessary.

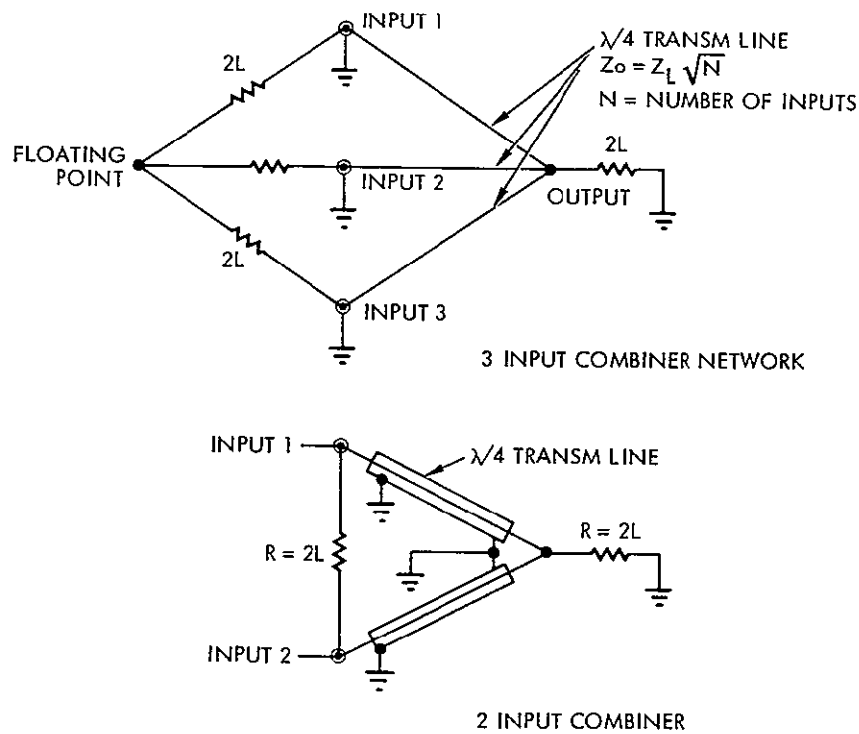

Figure 4. Power Combining Networks

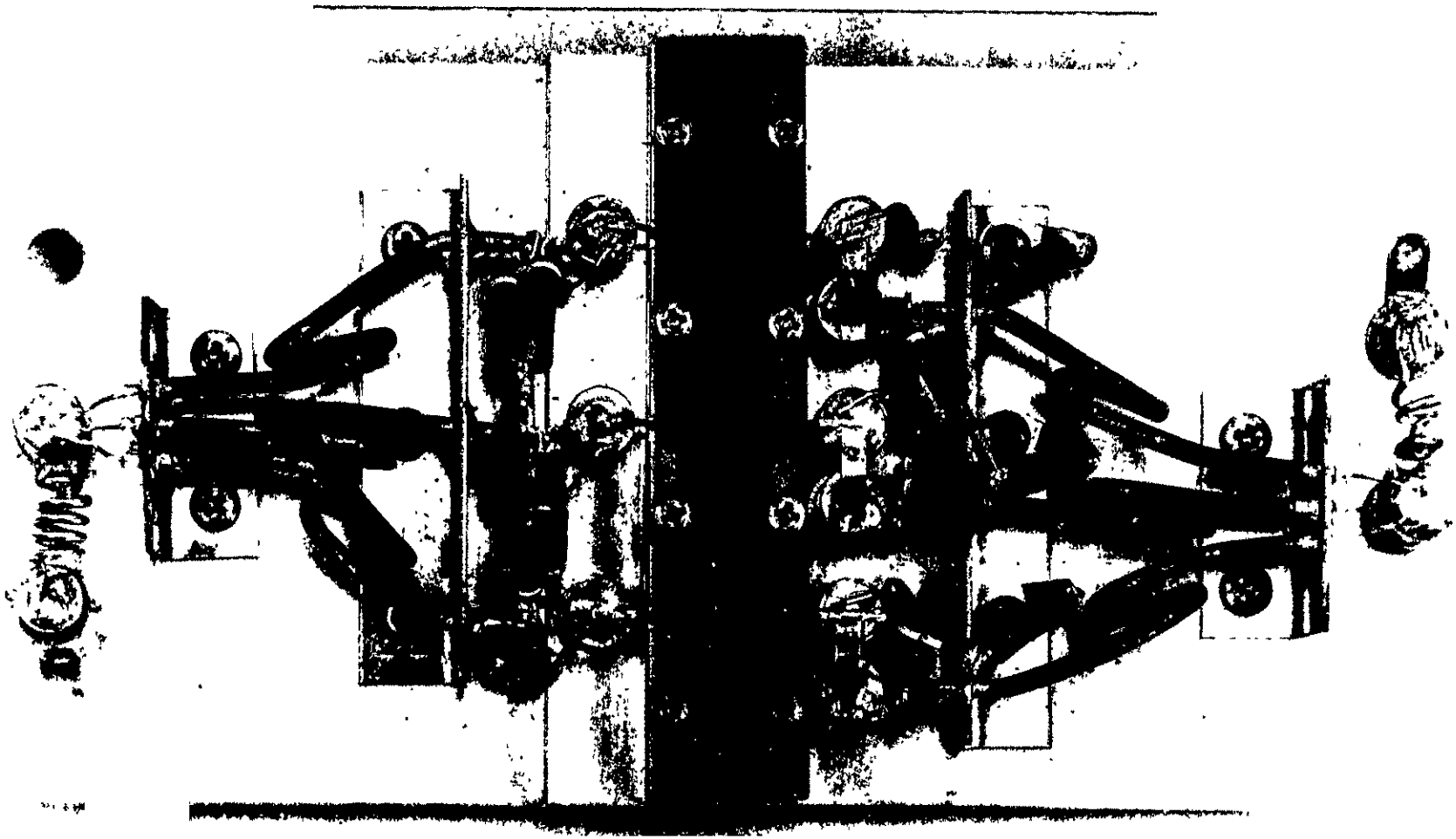

Figure 5. Test Prototype of Power Triplet

Table 2. Test Results on Triplet Unit

Transistor Number	Power Input (watts)	Power Output (watts)	$I_{28\ V}$ (amps)	Gain (db)	Efficiency (percent)
Individual Transistors					
1	7.8	20	1.0	4.1	71.5
2	7.7	20	0.9	4.1	79.0
3	6.8	20	1.0	4.7	71.5
Triplet Unit					
1, 2, 3	19.6	50	2.48	4.05	71.5

2.2 SOLID-STATE WITH L-BAND POWER AMPLIFICATION

The second solid-state design utilizes integrated circuit power modules operating directly at L-band and producing 20 watts maximum output power each. The modules do not exist at present but are projected to become available by mid 1969. This projection is based upon development at TRW Semiconductors on 10-watt integrated power chips operating at 2.0 GHz. Three new devices which will deliver 1.0, 2.5 and 5.0 watts at 2.0 GHz are now being introduced by TRW Semiconductors. Present plans are to emphasize development of increased power capability in the 1-2 GHz range rather than further extension of operating frequency at current power levels.

Appendix A shows a projection made by the U.S. Army Electronics Command on development of solid-state devices. This projection was made in July 1968 and indicates the development of transistors with CW power levels exceeding 10 watts above 1 gHz by 1972.

The concept for the transmitter is shown in Figure 6. The input from the phase modulator and driver is at 1560 MHz and requires only 63 milliwatts. The power amplifier is composed of 10-watt and 20-watt discrete integrated module stages and hybrid power dividing and combining units. The individual integrated amplifier modules utilize multi-transistor configurations on a single chip and microstriplines for internal matching and combining. Four 20-watt modules are shown for the output stage. The power per module is derated to keep the junction temperature below 125°C.

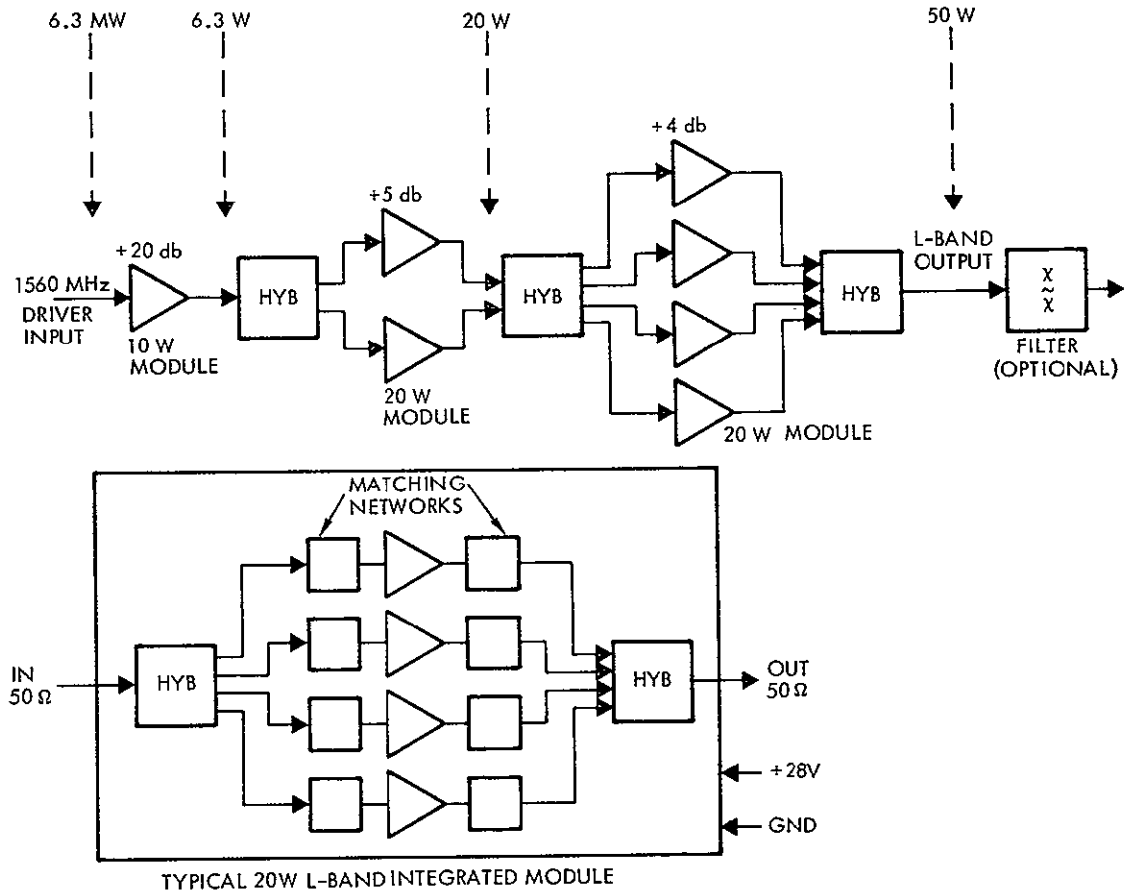

Figure 6. Design Concept for Direct L-Band Amplification Transmitter

With microstripline within the module, considerable reduction in lead length is achieved, increasing the operating frequency and power. Up to 15 watts at 2 GHz has been demonstrated using these techniques. The individual modules are designed with a 50-ohm input and output impedance so that their performance can be checked prior to integration into the system. The hybrid combiner and divider networks can also be constructed utilizing the stripline approach. Use of the stripline has an important advantage in that later mistuning of the networks is unlikely since distances once established will remain fixed.

This design seems more adaptable to 100 watts. The power can be extended by adding more modules in parallel. Matching and combining added units is not as serious a problem as for the first design because of the 50-ohm resistive input-output of each module and the microstripline.

The DC-to-RF efficiency for the 50-watt unit is estimated as follows. The DC power input to the power amplifier is

$$P_{dc} = \frac{P_o}{\gamma} \left[1 + \frac{1}{G_1} + \frac{1}{G_1 G_2} \right]$$

where

P_o = RF power output

γ = collector efficiency of each stage

G_1 = gain of final stage (4 db)

G_2 = gain of next stage (5 db)

The collector efficiency is conservatively estimated to be 46 percent. Overall efficiency of the power amplifier

$$\eta = \frac{P_o}{P_{dc}} = \frac{\gamma}{1 + \frac{1}{G_1} + \frac{1}{G_1 G_2}} \times 100 \text{ percent}$$

$$= 31 \text{ percent}$$

This efficiency depends primarily upon the power gain of the last stage. Therefore, particular attention will have to be paid to this area.

It is difficult to assess the size and weight of the power amplifier at this point, although it is anticipated that both will be significantly lower than possible with a discrete component design. As an example, a 5-watt module at 2.0 GHz measures 1.5" x 1.0" x 0.5".

Thermal resistance of these units is not known at this time, but good heat transfer from the active devices to the baseplate will be essential; hence a solid conducting mass for the housing will be required.

The following are the critical design areas for the power amplifier:

1) Since the present development on the high power modules is at S-band, scaling down will be required

2) Good familiarity with microstripline techniques will be necessary so that size and weight reduction can be achieved

3) Since maximum overall efficiency is a prime goal, considerable attention will be paid to the last power stage to optimize its performance

4) It is anticipated that a substantial effort will be spent in the area of thermal conductivity and interfacing to keep the junction temperature below 125°C.

2.3 TWT DESIGN

The third design of the transmitter uses a traveling wave tube operating at L-band to obtain 50 or 100 watts output. A phase modulator and driver nearly identical to that used with the second solid-state design is required. The driver output power is approximately 50 milliwatts for the 50-watt output, since a TWT typically has about 30 db gain.

The significant problem with this design is the availability of a space-qualified TWT for L-band application. Also the TWT requires an associated power supply or converter which generates all of the voltages to operate the tube from the primary +28V source.

Although considerable success has been obtained in the use of TWT transmitters for space applications, no TWT's at 50 or 100 watts at L-band have been flown.

Approximately two years ago, both Watkins-Johnson and Eimac (a division of Varian) embarked on a JPL-funded program to develop a 50-watt S-band TWT. The program is completed, and Eimac now claims to have a 50-watt S-band unit, and Watkins-Johnson a unit capable of both 50- and 100-watts at S-band. Although the units have wide bandwidths (nearly one octave) a "scaling down" redesign is necessary for L-band operation.

Both of the companies estimate that the scaling down would cost approximately $100-150K (6-9 months redesign time) which would be a nonrecurring cost. In addition, a space qualification cost would have to be added, approximately $100K, depending upon the requirements.

The units are designed specifically for space application with an intended lifetime of 50,000 continuous hours. Life expectancy at 90 per cent confidence level is estimated to be 20,000 hours. The size and weight of the redesigned S-band units would increase approximately by an amount proportional to the frequency difference.

2.4 COMPARISON OF SOLID-STATE AND TWT DESIGNS

The key parameters of the TWT and the first solid-state design are compared in Table 3. Realistic comparison with the second solid-state design are not possible because of the unknowns in the proposed devices. Preliminary indications of size, weight, and volume compare favorably with those shown in the table, and an expected DC-to-RF efficiency of at least 30 percent makes the second solid-state design attractive. Moreover, the use of integrated circuits and microstripline construction should result in its being the most reliable of the three.

The MTBF in the table are calculated in Appendix B. The calculations indicate that the solid-state transmitter using normal failure rates for the components has a higher MTBF than the TWT transmitter. It is perhaps worthwhile pointing out that the capacitor failure rate used in the solid state calculations occurred during alignment and test but not during orbital operations.

Table 3. Comparison of Transmitter Designs

Parameter	Solid-State (Design One)	TWT and Power Suppl (Converter)
Weight (pounds maximum)	6.0	8.5
Size (inches maximum)	12 x 5 x 2	15 x 6 x 4
Volume (cubic inches)	120	360
DC to RF efficiency (% minimum)	22	28
Bandwidth (%)	≤10	≥10
Gain in db (maximum)	As required	30 nominal
Power to weight ratio	8.3	5.9
Temperature range (^{o}C)	-20 to +65	-30 to +100
Vibration (operating)		20 g's, 20-2000 Hz
Shock (nonoperating)		200 g's, 1 msec
MTBF (hours)	39,200	32,400

A figure of merit based on the following formula:

$$\text{Figure of Merit} = \frac{\text{DC/RF eff. x MTBF}}{\text{weight x volume}}$$

shows an advantage of 4:1 for the solid-state design. This comparison is not totally fair since the parameters in the figure of merit are not of equal importance. For example, the overriding consideration in a choice may be the DC-to-RF efficiency since the satellite is power limited. However, the figure of merit does suggest the attractiveness of the solid-state design as compared to the TWT.

3. ULTRA-STABLE SATELLITE OSCILLATOR

It has been determined that a crystal reference oscillator will be adequate for the clock reference on each of the NAVSTAR satellites (see Appendix C). A crystal oscillator has physical characteristics which make it the most attractive unit for satellite application. In addition, the high initial cost and questionable reliability of atomic standards make the crystal oscillator even more attractive. Table 4 compares some of the characteristics of different oscillators. Although the figure of merit in the last column is somewhat arbitrary, nevertheless it suggests the attractiveness of the crystal oscillator.

Table 4. Comparison of Oscillator Characteristics

	Volume (ft^3)	Weight (lbs)	Power Consumption (watts)	Stability per 12 Hours	Figure of Merit (product of the four)
Atomic Hydrogen	16.4	800	200	2×10^{-14}	2.56×10^{-8}
Rubidium Gas Cell	0.5	38	42	5×10^{-12}	4.0×10^{-9}
Cesium Atomic Beam	1.5	64	60	2×10^{-13}	1.1×10^{-9}
Crystal Oscillator	0.082	6	2.5	1×10^{-11}	1.2×10^{-11}

A survey of companies that can produce the high precision crystal oscillators required for NAVSTAR indicates that few companies have built such units. Fortunately, one company has built an oscillator which appears to fit the NAVSTAR requirements and which has flown in space. A specification largely based on this oscillator has been written; a test program is recommended to confirm the performance of the oscillator.

3.1 CRYSTAL AGING

One of the main problems with crystal oscillators is the settling time or frequency stabilization when the oscillator is turned on. In general, frequency stabilization of a high quality oscillator follows a predictable curve. This stabilization is referred to as aging. However, it usually takes several months for a conventional oscillator to reach a stable frequency (Reference 2). Frequency stabilization with time follows a logarithmic law

$$\frac{\Delta f}{f}(t) = a + b \log_e \left[1 + \frac{t}{t_o}\right]$$

where a, b, and t_o are independent constants of the crystal. The aging rate is obtained by differentiating this expression

$$\frac{d}{dt}\left(\frac{\Delta f}{f}\right) = \frac{\frac{b}{t_o}}{1 + \frac{t}{t_o}}$$

Therefore as $t >> t_o$ the crystal frequency tends to stabilize. To minimize the settling time of the crystal t_o should be as short as possible.

Aging is considered to result primarily from mass loading changes on the quartz plate by the absorption of the contaminants that are trapped during the crystal mounting. Reduction in contaminants will decrease both the settling time and the magnitude of the aging.

Until recently, crystals have been encapsulated at normal temperatures, resulting in long stabilization periods. In addition, after equilibrium is reached and operation of the oscillator is interrupted, the aging time again follows the original characteristic (see Figure 7).

A new method utilizing a high temperature (400°C) hydrogen environment encapsulation has been developed to bake out the impurities. This reduces the contamination considerably, and reduces the aging from several months to a few weeks (see Figure 7). In addition, the reestablishment time of stable frequency after disruption is considerably

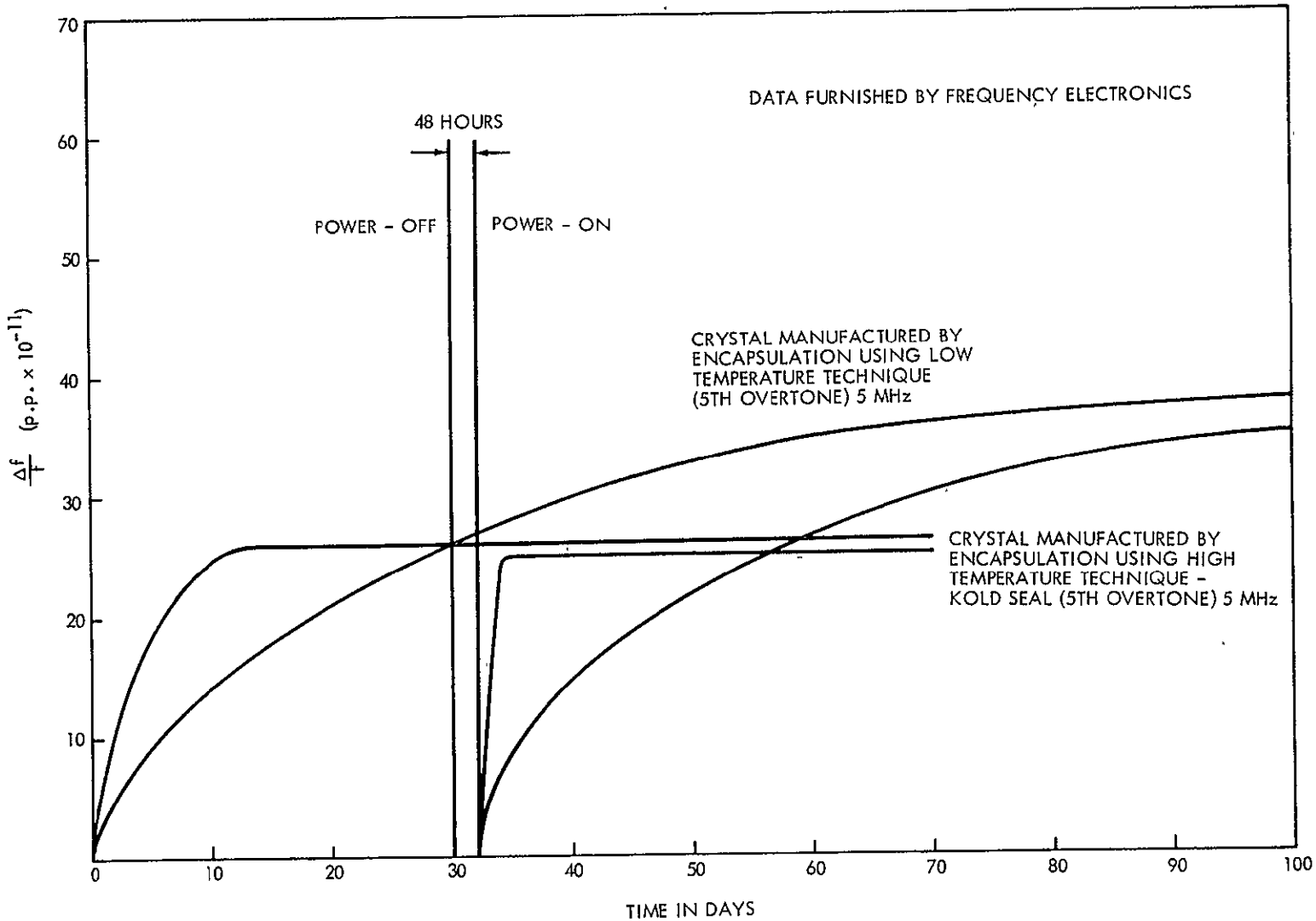

Figure 7. Aging Characteristics of Quartz Crystals

improved. The high temperature process is possible due to introduction of thermocompression bonding of the ribbons (the electrical contacts) to the quartz plate. Bake-out of solder-bonded units is limited to approximately 125°C.

With the present day crystal technology, a 5 MHz perpendicular field, fifth overtone crystal employing "Kold-seal" and thermocompression bonding is the best unit in terms of frequency and temperature stability. Also it is the least susceptible to mechanical shock and vibration.

3.2 CRYSTAL OSCILLATORS FOR NAVSTAR

Out of the companies surveyed involved in the design of high quality crystal oscillators, two were singled out on the basis of having demonstrated actual units flown in satellites: Applied Physics Laboratory, John Hopkins University, Maryland; and Frequency Electronics, Inc., New York.

The unit developed by the Applied Physics Laboratory was for the Dodge satellite. Its characteristics are as follows:

Operating frequency	5 MHz, fifth overtone horizontal field crystal supplied by Bliley Electric Company, utilizing conventional glass encapsulation
Temperature control	Double proportional oven
Aging rate	2×10^{-10} per day after 6 months of operation; 5×10^{-10} after 3 weeks of operation
Drift rate (rms)	2×10^{-10} per day 2×10^{-11} per 2000 second 1×10^{-10} per 200 second
Buss voltage sensitivity	2×10^{-11}/volt
Power consumption	1.5 watts
Ambient temperature sensitivity	$2 \times 10^{-11}/^{\circ}C$
Load resistance sensitivity	1×10^{-11}/ohm at 50 ohms

Load capacity sensitivity	2×10^{-11}/pf at 60 pf
Temperature range	-23 to +47°C
Weight	2.8 pounds
Dimensions	3.6 inches diameter x 5.0 inches high.

The above unit is not commercially available since it was designed under a Navy contract for a specific application. Actual in-flight data is not available. However, it is known that one of the units had a reported thermostat failure after four months of orbital operation. No remote frequency adjustment is provided. The price would be approximately $7-9K plus space qualification. The tests and delivery time would be approximately 6-8 months.

The unit designed by Frequency Electronics (Figures 8 and 9) was also developed for the Navy under USNRL Contract N00173-66-C-0162 and ONR Contract N0014-66-C-5220. The following are the unit's characteristics:

Operating frequency	5 MHz, fifth overtone horizontal field crystal, utilizing high temperature thermocompression bonding and "Kold-seal" encapsulation (the crystal is manufactured by the company)
Temperature control	Triple proportional oven
Aging rate	$1-2 \times 10^{-11}$ per day after 7 days of operation
Drift rate	$1-2 \times 10^{-11}$ per day $1-2 \times 10^{-12}$ per hour $4-8 \times 10^{-12}$ per second
Buss voltage sensitivity	1×10^{-11} for 5 percent voltage change
Power consumption	2.5 watts, including remote frequency control
Ambient temperature	1×10^{-12}/°C

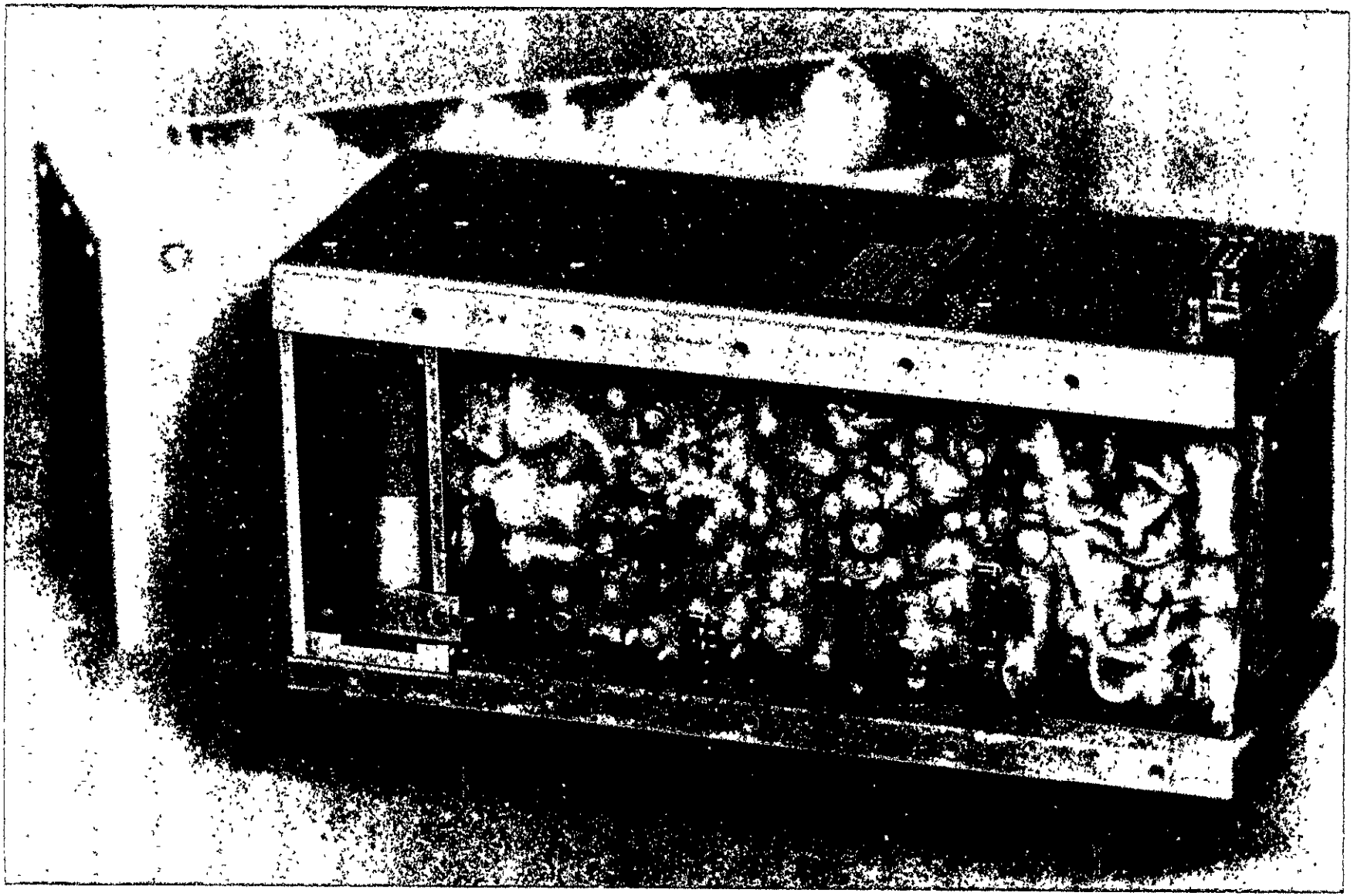

Figure 8. Frequency Electronics Crystal Oscillator

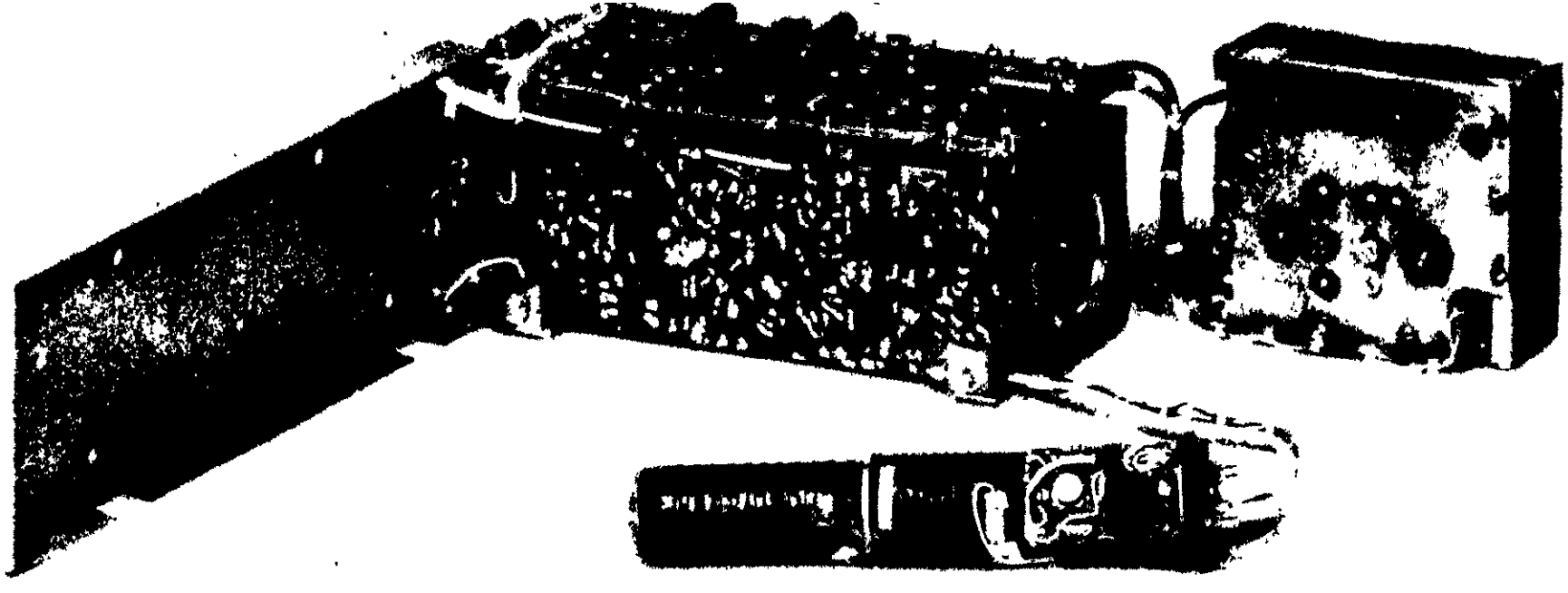

Figure 9. Frequency Electronics Crystal Oscillator

Load resistance sensitivity	1×10^{-11} for 20 percent load change
Remote frequency sensitivity	Utilizes mechanically variable capacitors, fine and coarse, adjustment by gear control unit Fine control resolution $\pm 1 \times 10^{-11}$ Coarse control range $\pm 2 \times 10^{-7}$ Control signal-digital
Temperature range	Present design of -20 to +45°C can be extended
Weight	4 pounds, 6.5 pounds with remote tuning
Dimensions	3.5 x 4.5 x 9.25 inches (with remote frequency control unit).

The design represents the state of the art for space-qualified high stability oscillators. The unit is commercially available, and the vendor is willing to cooperate in conducting additional tests. The price for an actual deliverable unit is shown below.

In quantities of two	Without remote frequency adjustment	— $ 8.0K each
	With remote frequency adjustment	— $11.5K each
	Space Qualification tests	— $12.0K

An oscillator built by Frequency Electronics for the Naval Air Systems Command was flown on an experimental satellite early in 1967. The 5 MHz oscillator frequency was counted down to 100 kHz and then used to modulate the 400 MHz carrier. The demodulated frequency was then compared to a 100 kHz hydrogen reference at the ground station. The oscillator which used a double proportional oven and a Bliley crystal, exhibited a temperature coefficient of approximately $1.7 \times 10^{-11}/^{\circ}C$, which since then has been improved to a $1 \times 10^{-12}/^{\circ}C$ by using a triple proportional oven. Figure 10 shows data obtained on the oscillator drift rate with time. The discontinuity at approximately 350 days is unexplained. Since this unit was flown considerable improvement in initial drift rate (aging) and vibration sensitivity has been made by improved crystal preparation methods.

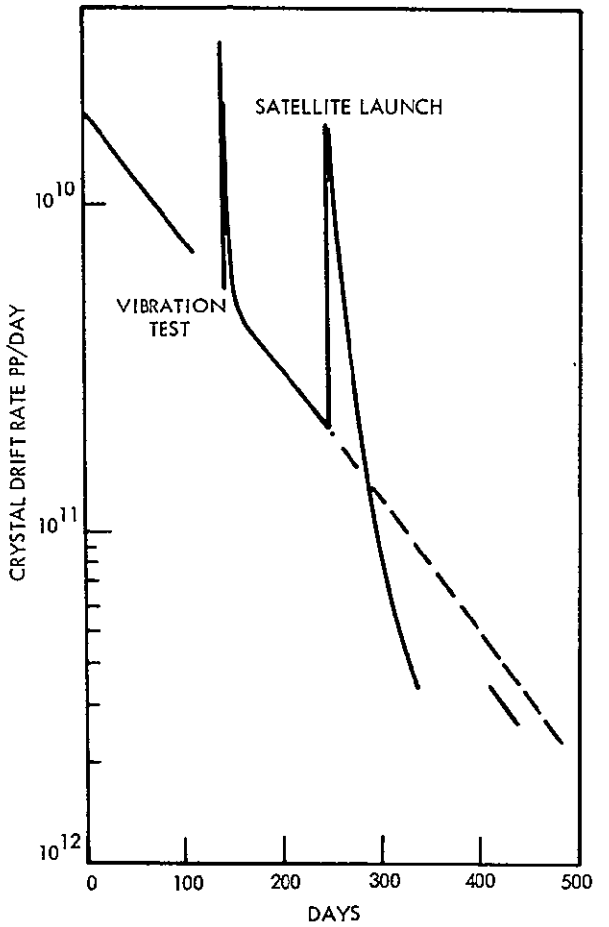

Figure 10. Oscillator Drift Rate Versus Time

3.3 RECOMMENDATIONS

The Frequency Electronics unit is recommended for use in a test program to evaluate the NAVSTAR application. It appears that the NAVSTAR requirements (see Table 5) can be met based upon data obtained from orbital flights and ground tests. The vendor claims that the final deliverable units can be reduced somewhat in size, and the temperature range can be extended. Presently the crystal is operating at an inflection point of approximately +60°C, where the aging rate is minimum. Operating the crystal at a higher temperature can be done at the expense of increased long-term drift.

The following tests should be performed on the oscillator:

1) General performance tests

   a) Output power
   b) DC power consumption
   c) Heater stability and thermal time constant

2) Output waveform evaluation using harmonic and spectrum analyses

   a) Harmonic content
   b) FM index using a multiplier in order to increase resolution

3) Stability measurements

   a) Phase stability - with an atomic standard reference using a high accuracy phase meter (measure time error against accumulated time with a resolution of at least 0.02μseconds)
   b) Frequency stability - by the use of multiplying chains and an atomic standard reference

4) Remote frequency correction evaluation including accuracy response and settling time

5) Environmental tests using the methods in 3 above

   a) Temperature
   b) Shock and vibration
   c) Sensitivity to power supplies and load impedance
   d) Humidity and pressure
   e) Radiation.

The phase stability measurements are of particular importance to obtain the proper oscillator error statistics for the NAVSTAR system. From these measurements "variate differences" can be derived, which are used to determine prediction error in the oscillator drift. See Appendix C for details on the variate difference measurements and their significance.

Table 5. NAVSTAR Specification for the Crystal Oscillator

Operating frequency	5 MHz
Frequency stability	1×10^{-12} per 3 hours
Aging rate	1×10^{-11} per day after 10 days of operation
Temperature sensitivity	$1 \times 10^{-12}/^{o}C$ or better
Buss voltage sensitivity	1×10^{-12}/1 percent voltage change
Power supply	$\pm$12V using 1 percent regulation
Power consumption	2.5 watts maximum
Ambient temperature	-10 to +55°C
Manual adjustment	Stability of 1×10^{-12}
Remote tuning (control signal to be specified later)	Fine tuning setability $\pm 1 \times 10^{-11}$ Coarse range $\pm 3 \times 10^{-7}$
Spurious outputs	Down not less than 80 db
Harmonics output	Down not less than 40 db
Vibration (exact specification to be supplied later)	The unit is to exhibit a stability of 1×10^{-8} during the launch period
Dimensions	4.0 x 5.0 x 10 inches maximum
Weight	6.5 pounds maximum, including remote tuning unit
EMI	To be specified
Humidity and pressure	To be specified

REFERENCES

1. TRW Systems, "Study of a Navigation and Traffic Control Technique Employing Satellites," Volumes I through IV, Contract NAS 12-539, Report 8710-6012-R000, December 1967.

2. J.A. Mullen, "Background Noise in Nonlinear Oscillators," Proceedings IRE, Volume 48(8), page 1467, 1960.

APPENDIX A

PROJECTION OF SOLID-STATE DEVICE DEVELOPMENT

by

U.S. Army Electronics Command

July 1968

U. S. ARMY ELECTRONICS COMMAND

Fort Monmouth, New Jersey

ELECTRONIC COMPONENTS LABORATORY

TECHNICAL GOALS AND PROJECTIONS

1 JULY 1968

TECHNICAL GOALS AND PROJECTIONS HAS BEEN PREPARED BY THE ELECTRONIC COMPONENTS LABORATORY AND IS PUBLISHED FOR THE INFORMATION AND GUIDANCE OF ALL CONCERNED. THE PROJECTIONS AND GOALS SHOWN ARE WHAT WE FEEL CAN BE ACCOMPLISHED IN VARIOUS MISSION RELATED SPECIALTY FIELDS IN THE TIME FRAMES INDICATED CONTINGENT UPON THE AVAILABILITY OF RESOURCES AND/OR PRIORITIES.

SOLID STATE DEVICES

This effort provides for the continuous exploratory development of solid state devices, including investigations of those materials and processing techniques which will lead to the development of advanced semiconductors or semiconductor-like devices.

Transistors & Diodes

The goals to be achieved in the discrete semiconductor device area include higher output powers from high frequency transistors, i.e., 200 to 500 watts PEP at 30 MHz, 50 to 100 watts at 500 MHz, and 25 watts at 1000 MHz. Three types of transistors are required; CW for FM operation, linear for single sideband use, and pulse for radar and pulse type communications. In the lower frequency semiconductor area audio units able to dissipate up to several kilowatts are required. In addition switching devices, which can switch several thousand amperes, will be developed for low voltage dc to dc converters and pulse modulators. High input impedance, linear, small-signal field effect transistors for front end receiver amplifier use ranging to microwave frequencies; and large signal, power (tens of watts) lower frequency field effect transistors will be developed.

Studies and ivestigations of improved semiconductor techniques, device improvement, new packaging concepts, and high power combining transistor circuit techniques will be advanced. They will include devices having higher breakdown voltages for AM applications in the UHF range; development of linear and varactor type transistors for SSB and frequency multiplication applications; development of long thermal time constant power transistor for pulse power applications, thereby hardening the device thermally to applied transients; investigations of laminated silicon transistors utilizing their smaller device geometries, and advantages of higher power capabilities, higher frequency responses, and higher breakdown voltages; the investigation of rate effects of four (4) layer structures; and low cost, low reactance packaging techniques, and evaluation.

The investigation of noise, its cause and theoretical behavior in new semiconductor devices applicable to military equipments, will be continued. In addition the internal work will continue with the goal of characterizing, evaluating and providing assistance in the application of new non-microwave, non-microelectronic semiconductor devices to military equipment. On the second graphic "TRANSISTORS - Power Output vs Frequency" the current curve indicates performance wherein power and frequency are limited, to a degree, by the material and processing methods. Future progress, i.e., through 1972, is based on the premise of an advanced state-of-the-art where optimum performance is obtained for silicon and new and more sophisticated processing techniques are utilized.

Unforeseen technological breakthroughs and new materials would make the prediction more optimistic.

The third chart also covers transistors. The power gains predicted for CW and SSB transistors are based on realistic "trade-offs" involving both frequency and efficiency; that is, increased power gain would result if lower efficiency were acceptable.

The field effect transistors, being essentially linear devices, will replace power vacuum tubes in SSB equipments at frequencies up to 76 MHz. Without unforeseen breakthroughs, higher frequency operation or powers in excess of 60 watts are not likely before FY-72.

SEMICONDUCTOR DEVICES

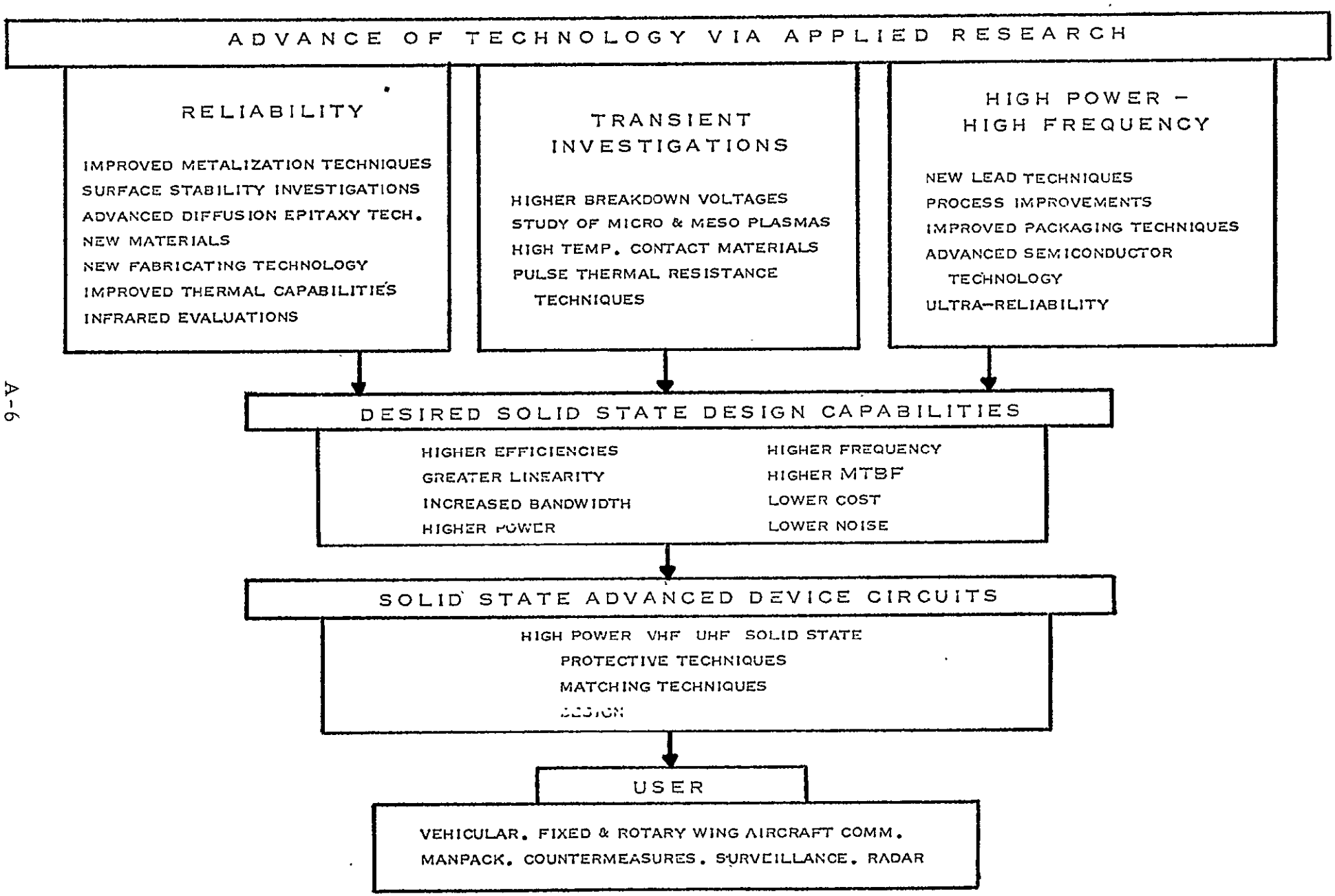

TRANSISTORS

POWER OUTPUT vs FREQUENCY

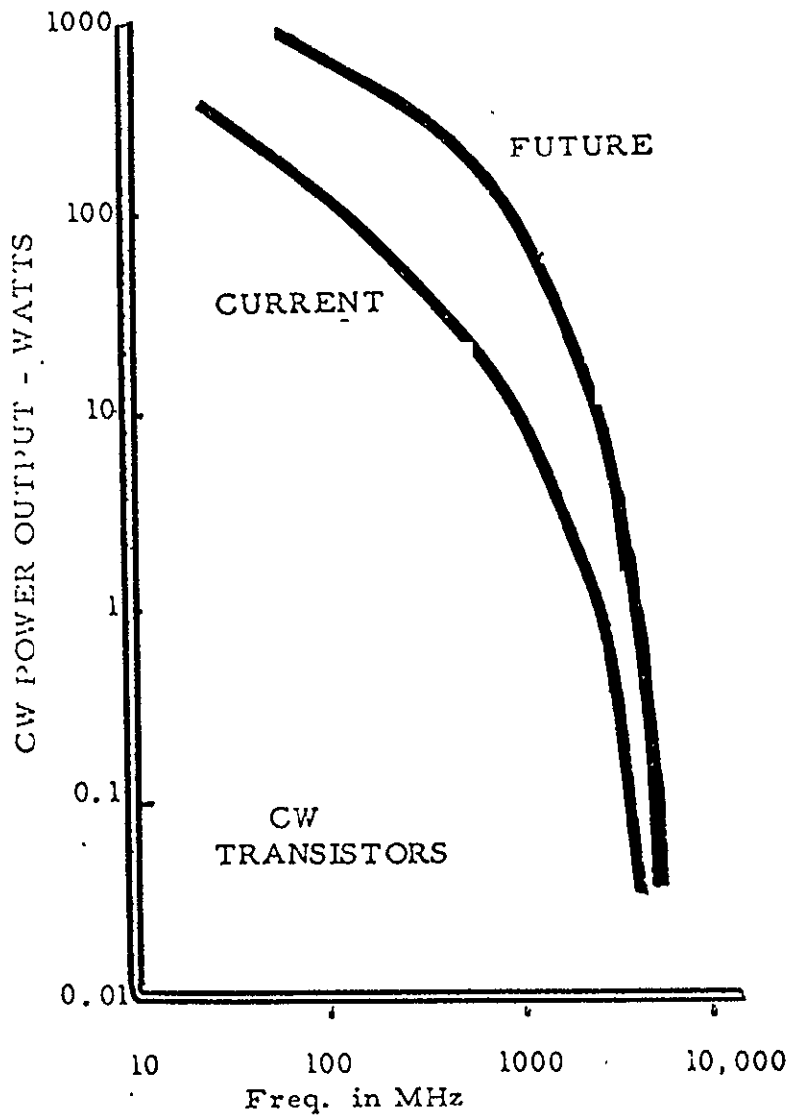

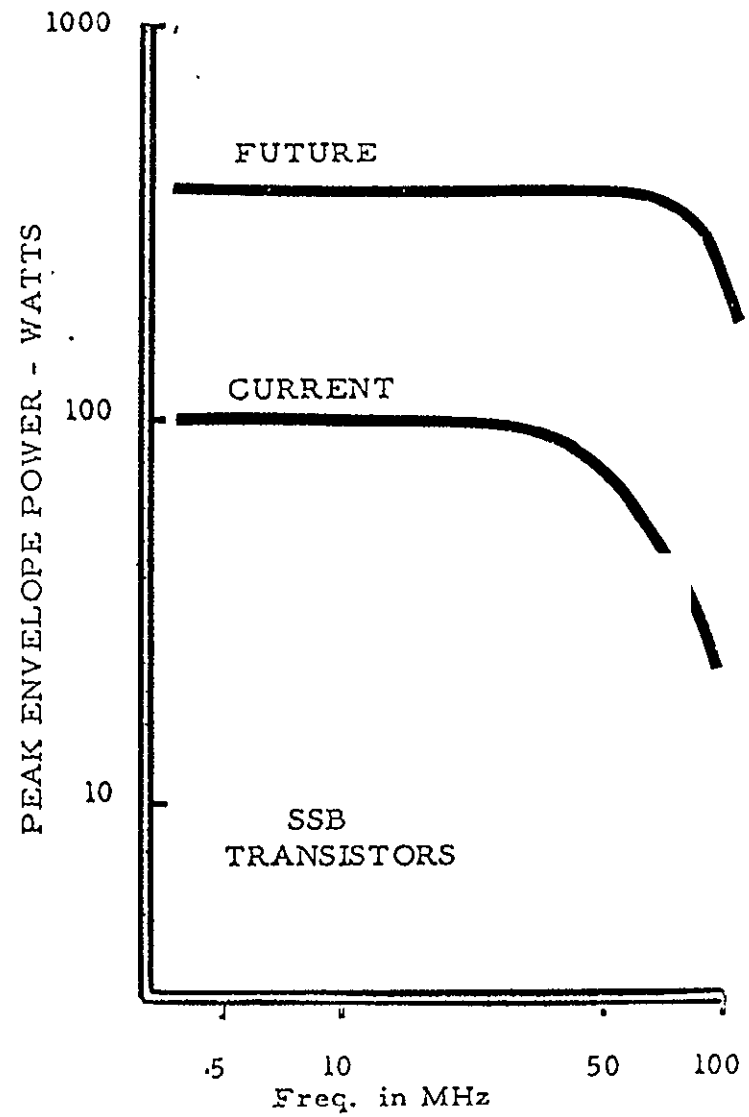

AV-545-68

TRANSISTORS

DEVELOPED — OBJECTIVE

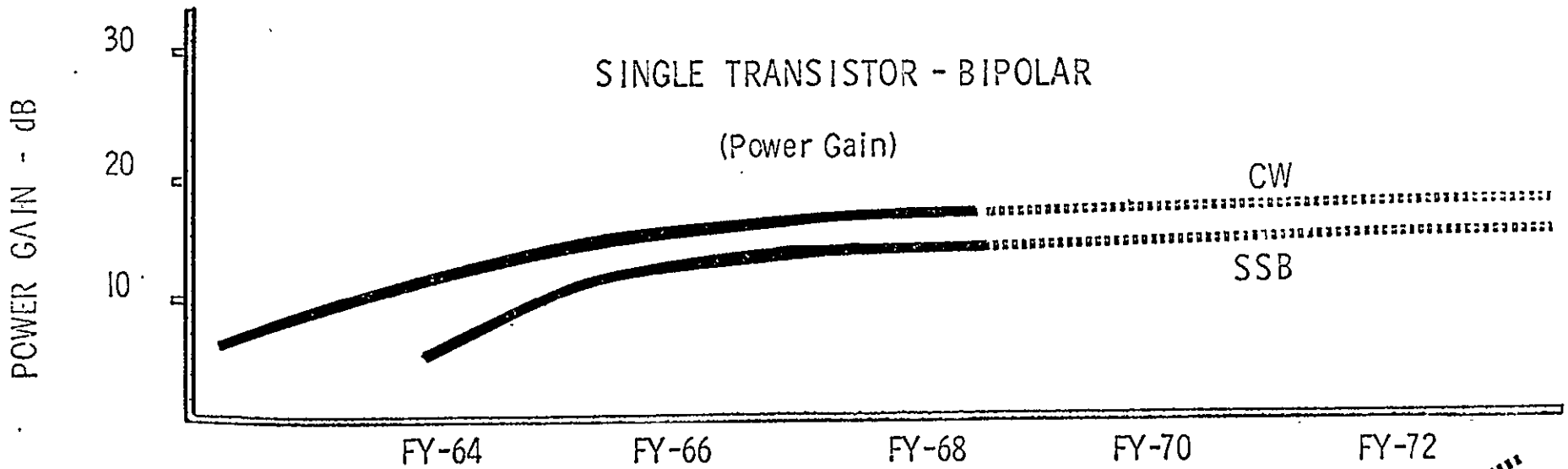

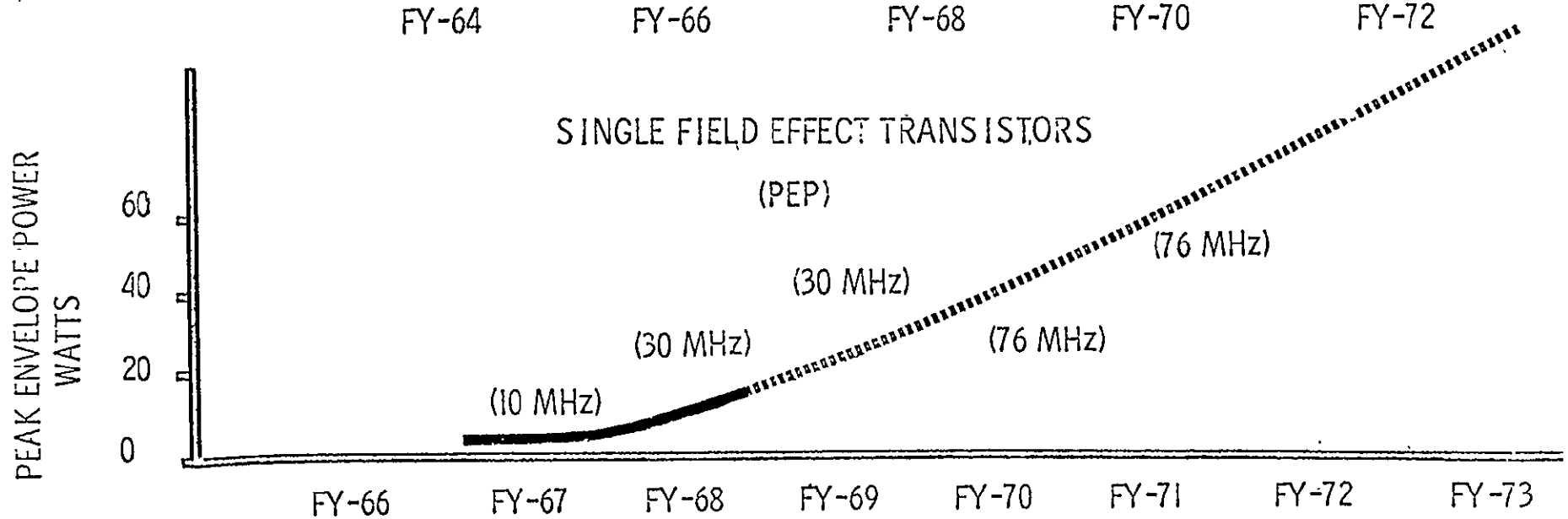

TRANSISTOR FAILURE RATE VS OUTPUT POWER

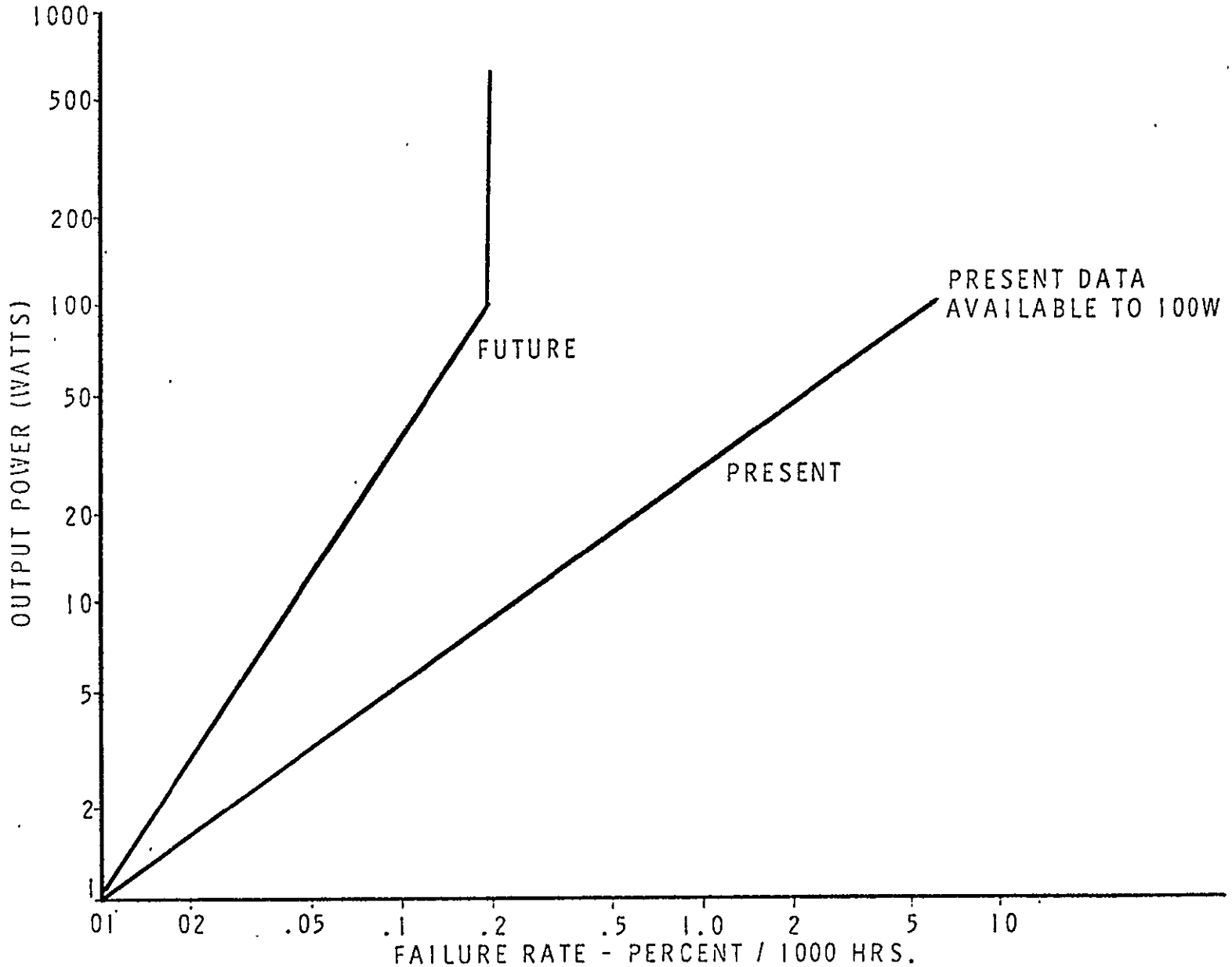

TRANSISTOR NOISE FIGURE VS FREQUENCY

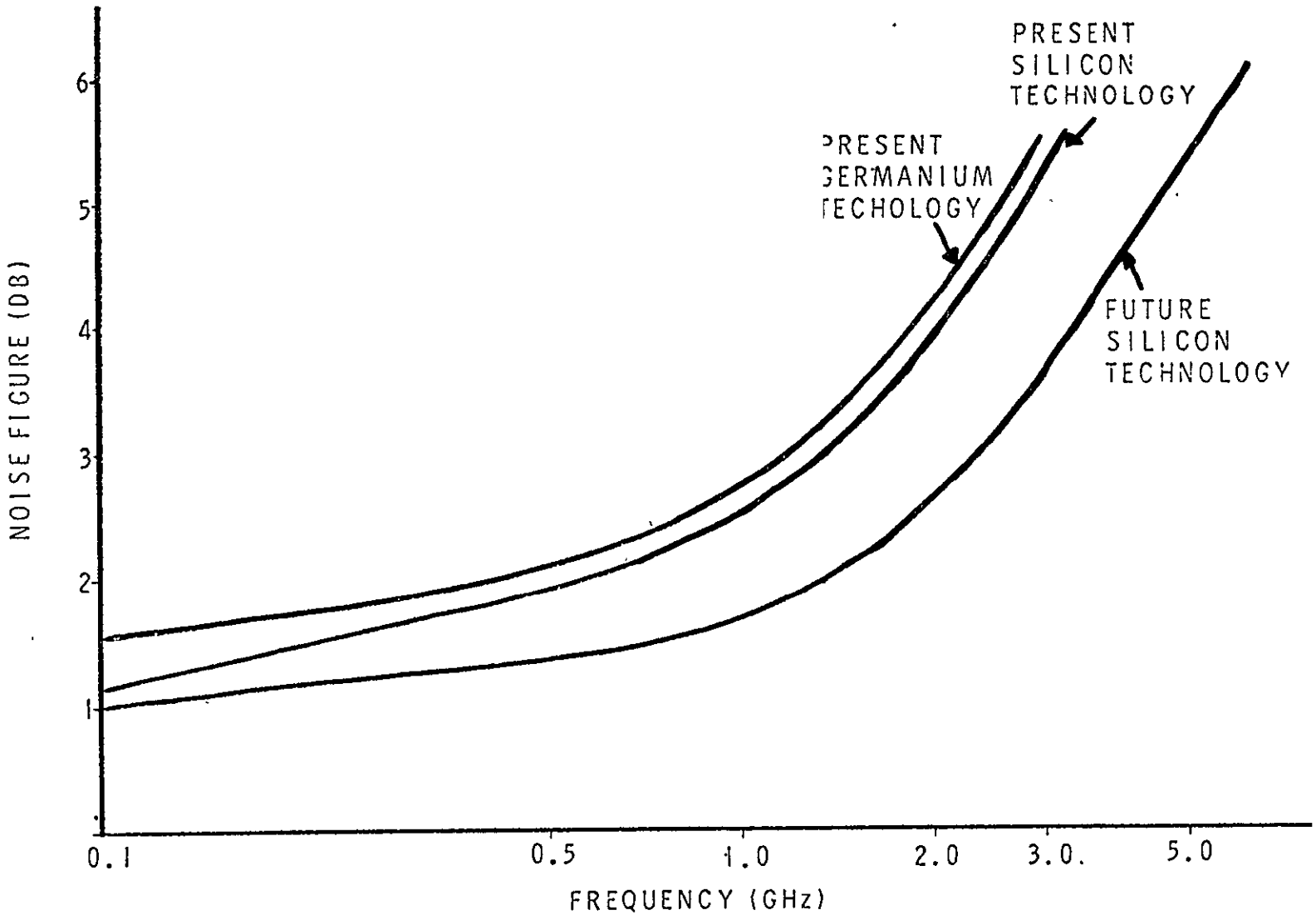

APPENDIX B

RELIABILITY CALCULATION FOR 50-WATT TWT AND SOLID STATE TRANSMITTER

Reliability predictions have been prepared for the 50-watt solid state transmitter (first design) to a 50-watt TWT and its converter. The results are presented in Table B-1. Table B-2 lists the failure rates for each part used in the predictions. Most of these failure rates are based on orbital operating hours accumulated by the OGO, Vela, and Pioneer Spacecraft. The low failure rate for power transistors is the maximum likelihood estimator based on the number of failures and part hours. The high failure rate for power transistors is the upper one-sided confidence limit at 60 percent confidence level. The low failure rate for variable capacitors is based on engineering judgement since it is a low usage part and has not accumulated many orbital hours. The high failure rate for variable capacitors is the upper one-sided confidence limit at 60 percent confidence level. The failure rate for the 50-watt TWT was supplied by the Eimac Division of Varian Associates. TRW has no orbital data on TWT's of this power rating.

All failure rates were adjusted by a computer program (TESRX) for the principal electrical stress and temperature on each particular part. The program adjusts the failure rates by means of a four-parameter Eyring model which has been fitted to the temperature-stress curves of MIL-HDBK-217A for each generic part type.

To predict the reliability of a 50-watt TWT and converter, it was necessary to obtain a parts count for a typical TWT converter. The TWT converter in the Pioneer spacecraft was selected.

To provide a range of values, three predictions were prepared using three different part case temperatures, 50°C, 60°C, and 70°C. For each prediction, the principal electrical stress on the parts was assumed to be 30 percent on semiconductors, 50 percent on solid tantalum capacitors, 25 percent on the other types of capacitors, and 25 percent on resistors. These values were selected as typical stress levels based on other TRW designed converters. The parts count and failure rates are listed in Table B-3. The results indicate a range from 28,600 to 32,400 hours MTBF for the TWT and converter.

Table B-1. Predicted MTBF's

	Failures Per 10^9 hours	MTBF = Mean Time Between Failures (hours)
TWT and Converter		
At 50°C Case Temperature	30,887	32,400
At 60°C Case Temperature	32,793	30,500
At 70°C Case Temperature	35,013	28,600
Solid State Transmitter		
With low failure rates for variable capacitors and rf power transistors.	20,129	49,700
With low failure rate for variable capacitors and high failure rate for rf power transistors.	25,524	39,200
With high failure rate for variable capacitors and low failure rate for rf power transistors.	46,979	21,300
With high failure rates for variable capicators and rf power transistors.	52,374	19,100

Table B-2. Part Failure Rates

Part Type	Failures/10^9 Hours at 25% Stress and 30°C	
Diodes		
Varactor	276	
Silicon Power	14	
Zener	60	
Transistor		
Silicon Power	560	863
Resistor		
Carbon Composition	7	
Metal Film	1.4	
Wirewound	65	
Capacitor		
Ceramic	15	
Mica, dipped	3	
Glass	23	
Tantalum Solid	14	
Variable	40	219
Transformer		
Low Voltage	15	
High Voltage	30	
Inductor	15	
Traveling Wave Tube (TWT), 50 watt	20,000	

Table B-3. TWT and Converter

Part Type	Quantity	Total Stressed Failure Rate Failures/10^9 Hours		
		At 50°C Case Temperature	At 60°C Case Temperature	At 70°C Case Temperature
Diodes, silicon power	48	1008	1152	1344
Diodes, zener	3	270	312	360
Capacitors, solid tantalum	13	667	867	1022
Capacitors, ceramic	7	168	238	336
Capacitors, mica	1	2	3	3
Capacitors, glass	4	192	296	448
Resistors, carbon comp.	15	300	540	930
Resistors, metal film	11	22	22	22
Resistors, wirewound	1	69	74	79
Transistors, silicon power	10	7970	9070	10, 250
Inductors	5	75	75	75
Transformers, low voltage	3	45	45	45
Transformers, high voltage	3	90	90	90
Traveling Wave Tube (TWT)	1	20, 000	20, 000	20, 000
TOTAL		30, 878	32, 784	35, 004

Note: The following principal electrical stress levels were assumed for this prediction:

Semiconductors — 30%
Capacitors, solid tantalum — 50%
Capacitors, all other types — 25%
Resistors — 25%

The case temperatures of the parts will depend on the baseplate temperature and the packaging technique. A tightly packed unit will cause higher case temperatures since less space is available for heat dissipation and vice versa.

The block diagram for the solid-state amplifier is shown in Figure 2 and the schematics of the amplifier stages and hybrids are shown in Figures 3 and 4.

For this prediction, a baseplate temperature of 50°C was specified. The electrical stresses on the semiconductors were calculated using the power levels given in Figure 2. An electrical stress of 25 percent was assumed for all other parts. Four predictions were prepared by using the two different failure rates for power transistors and variable capacitors discussed above.

The power transistors proposed for the transmitter are new high frequency, high power devices. There is no data available to indicate the reliability of these devices. Therefore the low and high failure rates were selected to provide a range of predictions. The low failure rate would apply to transistors procured with a complete parts control program and the high rate would apply if there was a limited program. In either case the transistors would require PT specifications and qualification testing.

The variable capacitors have not accumulated many orbital hours and therefore have a high failure rate at the 60 percent confidence level. The low failure rate is typical of what has been used in reliability predictions for other programs at TRW.

The parts count and stressed failure rates are listed in Table B-4. The results indicate a range from 19,000 to 49,700 hours MTBF for the solid-state transmitter.

The solid state transmitter can be made more reliable by reducing the number of variable capacitors, replacing some of the variable capacitors with fixed capacitors, or controlling the reliability level of the variable capacitors by instituting a complete parts control program.

The tuning procedure required for the solid-state transmitter could affect the reliability of the variable capacitors. Problems have been encountered on other programs at TRW. When the variable capacitors were adjusted too frequently, the movable parts became worn and loose and had to be replaced. It was necessary to limit the number of adjustments which could be made to the variable capacitors. If this transmitter is expected to have a long repetitive tuning procedure, steps should be taken to prevent this problem with the variable capacitors.

Table B-4. Solid State Transmitter

Part Type	Quantity	Total Stressed Failure Rate (Failures/10^9 Hours) at 50° Baseplate Temperature			
		Low Capacitor Low Transistor	Low Capacitor High Transistor	High Capacitor Low Transistor	High Capacitor High Transistor
A1 Amplifier stage	1				
Transistor, power (PT6680)	1	489	754	489	754
Capacitor, variable	5	400	400	2, 190	2, 190
Capacitor, ceramic	2	48	48	48	48
Inductor	4	60	60	60	60
A2 Amplifier stage	2				
Transistor, power (2N5177)	1	638	983	638	983
Capacitor, variable	5	400	400	2, 190	2, 190
Capacitor, ceramic	2	48	48	48	48
Inductor	4	60	60	60	60
A3 Amplifier stage	2				
Transistor, power (2N5177)	2	1, 504	2, 318	1, 504	2, 318
Capacitor, variable	10	800	800	4, 380	4, 380
Capacitor, ceramic	4	96	96	96	96
Inductor	8	120	120	120	120
A4 Amplifier stage	2				
Transistor, power (2N5178)	3	2, 598	4, 004	2, 598	4, 004
Capacitor, variable	15	1, 200	1, 200	6, 570	6, 570
Capacitor, ceramic	6	144	144	144	144
Inductor	12	180	180	180	180
x 3 Multiplier	2				
Diode, varactor	2	1, 270	1, 270	1, 270	1, 270
Capacitor, variable	5	400	400	2, 190	2, 190
Inductor	4	60	60	60	60
Hybrid (2:1 or 1:2)	6	24	24	24	24
Hybrid (3:1 or 1:3)	4	32	32	32	32
Miscellaneous resistors, metal film	20	40	40	40	40
Total		20, 129	25, 524	46, 979	52, 374

NOTES: The electrical stresses on the semiconductors were calculated using the power levels given in Figure 2
A principal electrical stress of 25 percent was assumed for all other parts

The specifications from Eimac for the 50-watt TWT include a design life of 20,000 hours. Therefore, for this prediction (28,600 to 32,400 hours MTBF for TWT and converter), it was assumed that the TWT would not be operated continuously for more than 20,000 hours during a mission.

APPENDIX C

OSCILLATOR ERROR STATISTICS FOR NAVSTAR

Introduction

This appendix summarizes the available information on very stable oscillators pertaining to the question of oscillator error in what may be called the "autonomous" mode of NAVSTAR operation.

In this mode, the satellite transmissions originate at the satellite independently or autonomously by reference to very stable oscillators on the satellites as opposed to retransmission of signals from the ground. The satellite signals are received at a number of fixed ground stations at known locations whose observations are then used to estimate a "total ephemeris" consisting of satellite position and velocity elements and satellite oscillator bias and one or more oscillator bias rate terms. This total ephemeris is then broadcast to all users to allow them to correct for differences in satellite oscillators. The bias corrected data is then equivalent to fully synchronized satellite transmission.

To determine optimum bias estimation time constants, ephemeris update periods, and the net effect on user position error it is necessary to characterize the time serial statistics of the random oscillator drift.

Practical considerations of satellite hardware weight, simplicity, and reliability have led to an emphasis on the crystal and rubidium oscillators so only these two types are considered here.

Oscillator Error Characterization

Consider an oscillator (or clock) providing a phase (or indicated time)

$$\phi(t)$$

Relative to a given reference oscillator of frequency ω_o (which defines ω_o) we can measure the phase error

$$\phi^*(t) = \phi(t) - \omega_o t \tag{1}$$

$\phi^*(t)$ may be characterized as a random time varying phase error. In order to normalize things it is convenient to define the indicated time error

$$t^*(t) = \frac{\phi^*(t)}{\omega_o} \tag{2}$$

and the associated range error in a system using this as a range delay measuring reference

$$\rho^*(t) = c\,t^*(t) \tag{3}$$

where c is the velocity of light $\approx 10^9$ ft/sec.

Several relatable measures of the essential statistics of these three equivalent random functions are in common use.

1. Short Time Frequency Stability

The change in phase error in a time τ, divided by τ is a measure of the frequency error over τ, thus

$$\omega_t^*(t) = \frac{\phi^*(t-\tau) - \phi^*(t)}{\tau}$$

If one measures $\omega_t^*(t)$ in N contiguous intervals

$$\omega_\tau^*(t_o)$$

$$\omega_\tau^*(t_o + \tau)$$

$$\vdots$$

$$\omega_\tau^*\Big(t_o + (N-1)\tau\Big)$$

forms the sample mean

$$\overline{\omega_N^*}(t_o) = \frac{1}{N} \sum_{i=0}^{N-1} \omega_\tau^*(t_o + i\tau)$$

$$= \omega_{N\tau}^*\left(t_o + (N-1)\tau\right)$$

forms the residuals relative to that mean

$$\Delta\omega^*(t_o + i\tau, N) = \omega_\tau^*(t_o + i\tau) - \overline{\omega_N^*(t_o)}$$

and the rms residual

$$S(\tau, N) = \left[\frac{1}{N-1} \sum_{i=0}^{N-1} \Delta\omega^{*2}(t + i\tau)\right]^{1/2} \tag{4}$$

Then $S(\tau, N)$ is the commonly measured short time stability of the oscillator.

2. Spectrum

Considered as a random function of time $\phi^*(t)$ (or equivalently t^* or ρ^*) may be characterized in terms of its power spectral density function

$$G_\phi(f)$$

or its autocorrelation function

$$R_\phi(\tau)$$

which by the Wiener-Khintchine theorem is just the Fourier transform of $G_\phi(\tau)$. Usually these are both singular forms since in actuality the zero values of both of these functions are infinite. If one is careful however, this does not necessarily interfere with their formal usage in analysis since the expressions one usually wishes to evaluate in terms of G or R are usually finite, i.e., independent in an appropriate sense of the zero frequency values of G or R.

3. Variate Differences

Given a series of values of ϕ^* at intervals τ

$$\phi^*(t_o)$$

$$\phi^*(t_o + \tau)$$

$$\vdots$$

$$\phi^*(t_o + i\tau)$$

$$\vdots$$

form the successive differences

$$\Delta_\phi^{(1)}(t_o + i\tau) = \phi^*(t_o + i\tau) - \phi^*\Big(t_o + (i-1)\tau\Big)$$

$$\Delta_\phi^{(2)}(t_o + i\tau) = \Delta_\phi^{(1)}(t_o + i\tau) - \Delta_\phi^{(1)}\Big(t_o + (i-1)\tau\Big)$$

etc.

and the means $\overline{\Delta_\phi^{(j)}}$ and variances

$$\sigma_\phi^{(j)^2}(\tau) = \left\langle \left[\Delta_\phi^{(j)}(t_o + i\tau) - \overline{\Delta_\phi^{(j)}} \right]^2 \right\rangle \tag{5}$$

Depending somewhat on the type of oscillator the variance of ϕ^* itself (i.e., $\sigma_\phi^{(o)^2}$) and $\sigma_\phi^{(1)^2}$ are generally indeterminate but $\sigma_\phi^{(2)^2}$ and all higher order differences generally exist and are finite.

Relations Between the Various Statistics

Because of the singularity of some of the functions otherwise involved, a useful place to start is in terms of the "structure functions,"

$U(\tau)$ defined as the mean square difference of phase (or time, or range) samples τ apart

$$U(\tau) = \left\langle \left[(\phi^*(t+\tau) - \phi^*(t) \right]^2 \right\rangle$$

This can be directly related to the autocovariance function, $R(\tau)$ <u>if</u> the latter exists through expanding

$$U(\tau) = \left\langle \phi^{*2}(t+\tau) \right\rangle + \left\langle \phi^{*2}(t) \right\rangle$$

$$- 2 \left\langle \phi^*(t)\, \phi^*(t+\tau) \right\rangle$$

$$= 2 \left[R(0) - R(\tau) \right]$$

$$R(\tau) = R(0) - \frac{U(\tau)}{2}$$

Further it can be shown (Ref. 2), from the preceeding definitions that

$$S^2(\tau, N) = \frac{1}{(N-1)\tau^2} \left[N\,U(\tau) - \frac{1}{N} U(N\tau) \right]$$

and

$$\Delta^{(2)^2}(\tau) = 6R(0) - 8R(\tau) + 2R(2\tau)$$

$$= 4U(\tau) - U(2\tau)$$

$$\Delta^{(3)^2}(\tau) = 20R(0) - 30R(\tau) + 12R(2\tau) - 2R(3\tau)$$

$$= 15U(\tau) - 6U(2\tau) + U(3\tau) \qquad \text{etc.}$$

and finally the phase spectrum is given (if it exists):

$$G_\phi(f) = 4\int_0^\infty R(\tau)\cos 2\pi f\tau\, d\tau$$

$$= 2R(0)\,\delta(f) - 2\int_0^\infty U(\tau)\cos 2\pi f\tau\, d\tau$$

and ignoring the D.C. term we may write

$$G_\phi(f) = -2\int_0^\infty U(\tau)\cos 2\pi f\tau\, d\tau \qquad (f \neq 0)$$

General Power Law Models

It turns out both experimentally and theoretically that over wide ranges of frequency the various functions above may be represented as simple powers of their arguments. Thus if we set

$$U(\tau) = K\tau^v$$

we have from the above relations

$$S^2(\tau, N) = \frac{NK\tau^{v-2}}{N-1}\left[1 - N^{v-2}\right]$$

$$\Delta^{(2)^2}(\tau) = K\tau^v\left[4 - 2^v\right]$$

$$\Delta^{(3)^2}(\tau) = K\tau^v\left[15 - 6\cdot 2^v + 3^v\right]$$

$$G_\phi(f) = -2K\int_0^\infty \tau^v\cos 2\pi f\tau\, d\tau$$

$$G_\phi(f) = -\frac{K\pi}{\Gamma(-v)\cos\frac{v\pi}{2}\,(2\pi)^{v+1} f^{v+1}}$$

$$= \frac{2K\,\Gamma(1+v)\sin\frac{\pi v}{2}}{(2\pi)^{v+1} f^{v+1}}$$

Particular Power Laws

Particular cases of interest are

$v = -1$ corresponding to phase modulation by white noise

$v = 1$ corresponding to frequency modulation by white noise

$v = 2$ corresponding to frequency modulation by $1/f$ or "flicker" noise

The first case ($v = -1$) leads to indeterminate relations between the various measures, and in fact, only G is defined in this case since the mean square phase jitter or phase jitter differences of any order are infinite. In practice this indeterminacy is resolved by finite circuit bandwidths which circumvent the implied ultraviolet catastrophy (Ref. 1). However, the details of this resolution need not concern us here since over the time constants and frequencies of interest in the NAVSAT problem (i.e., $\tau >> 1$ sec) this type of noise is generally not significant.

The second case ($v = 1$), corresponding to white noise frequency modulation, gives ($v = 1$)

$$S^2(\tau, N) = \frac{K}{\tau} \text{ (independent of } N)$$

$$\Delta^{(2)^2}(\tau) = 2K\tau$$

$$\Delta^{(3)^2}(\tau) = 6K\tau$$

$$G_\phi(f) = \frac{2K}{(2\pi)^2 f^2}$$

The third case ($v = 2$) corresponds to flicker frequency modulation and is of particular interest since it seems that all oscillators, with the possible exception of the maser class, approach such a characteristic asymptotically for long times or low frequencies. All the general power law relationships above unfortunately go to zero. However, this does not correspond to any real physical blow-up, and in fact the ratio of the various functions approaches a constant as v approaches 2, which ratio may be evaluated by L'Hospitals rule. Normalizing with respect to, say arbitrarily, the term $4 - 2^v$ we have in the limit $(v \to 2)$

$$S^2(\tau, N) = \frac{KN}{N-1}\left(\frac{1 - N^{v-2}}{4 - 2^v}\right) \to \frac{KN}{4(N-1)}\left(\frac{\ln N}{\ln 2}\right)$$

$$\Delta^{(2)^2}(\tau) = K\tau^2$$

$$\Delta^{(3)^2}(\tau) = K\tau^2\left[\frac{15 - 6\cdot 2^v + 3^v}{4 - 2^v}\right] \to K\tau^2\left[\frac{24\ln 2 - 9\ln 3}{4\ln 2}\right]$$

$$G_\phi(f) = \frac{4K}{(2\pi)^3 f^3}\left[\frac{\sin\frac{\pi v}{2}}{4 - 2^v}\right] \to \frac{K\pi}{(2\pi)^3(2\ln 2)f^3}$$

These numerical relationships are summarized below.

v	$G_\phi(f)$	$G_\omega(f)$	$\Delta^{(2)^2}(\tau)$	$\Delta^{(3)^2}(\tau)$	$S^2(\tau, N)$
1	$\frac{2K}{(2\pi)^2 f^2}$	$2K$	$2K\tau$	$6K\tau$	$\frac{K}{\tau}$
2	$\frac{K}{109 f^3}$	$\frac{K}{2.78 f}$	$K\tau^2$	$2.43K\tau^2$	$\frac{K}{2.78}\left(\frac{N\ln N}{N-1}\right)$

Comparison of Actual Data

Figure C-1 is a composite plot of several short time frequency stability plots for several crystal and one rubidium oscillator from the sources indicated. Based on such data and also on McCoubrey's (Ref. 5) characterization, we propose to approximate these diverse ensembles by the generic representations of Figure C-2. These can be easily transformed into the spectral domain by the relations previously derived and lead to the effective velocity (proportional through $c^2 = (0.983 \cdot 10^9)^2$ to relative frequency) error spectra as shown on Figure C-3. The quartz oscillators at relatively high frequencies show the up-turn spectrum effect of white noise phase modulation, introduced through relations derived in Reference 1 and assuming a respective 160 Hz noise bandwidth; but this is really not essential to the present discussion since it only affects frequencies above about 1 Hz.

At low frequencies both quartz and rubidium show the characteristic 1/f or flicker frequency or velocity spectra, the rubidium having a very slight advantage for frequencies below about 0.001 Hz (with one exception to be discussed).

A major difficulty of the usual short-time stability function at very long times concerns the methods of eliminating trends and the dependence on N. Usually insufficient attention is paid to these details and the reported results are somewhat deteriorated for lack of reporting of these necessary details. Recognizing these limitations, Barnes (Ref. 3) has proposed and utilized the short term variate difference—variance as a better behaved statistic. Figure C-4 shows the rms or standard deviation of variate differences of various orders for a cesium and a quartz oscillator. Over the range or values plotted σ varies as τ for the quartz oscillator implying a phase jitter spectrum of the form f^{-3} or "flicker" noise in frequency.

Again the previously derived results permit inferring the frequency or velocity error spectra from the preceding results and this is also plotted on Figure C-3. It is seen that this oscillator is nearly an order of magnitude better than the proposed (Ref. 6) generic characterization for quartz oscillators. Several factors may be brought forth to account for this difference.

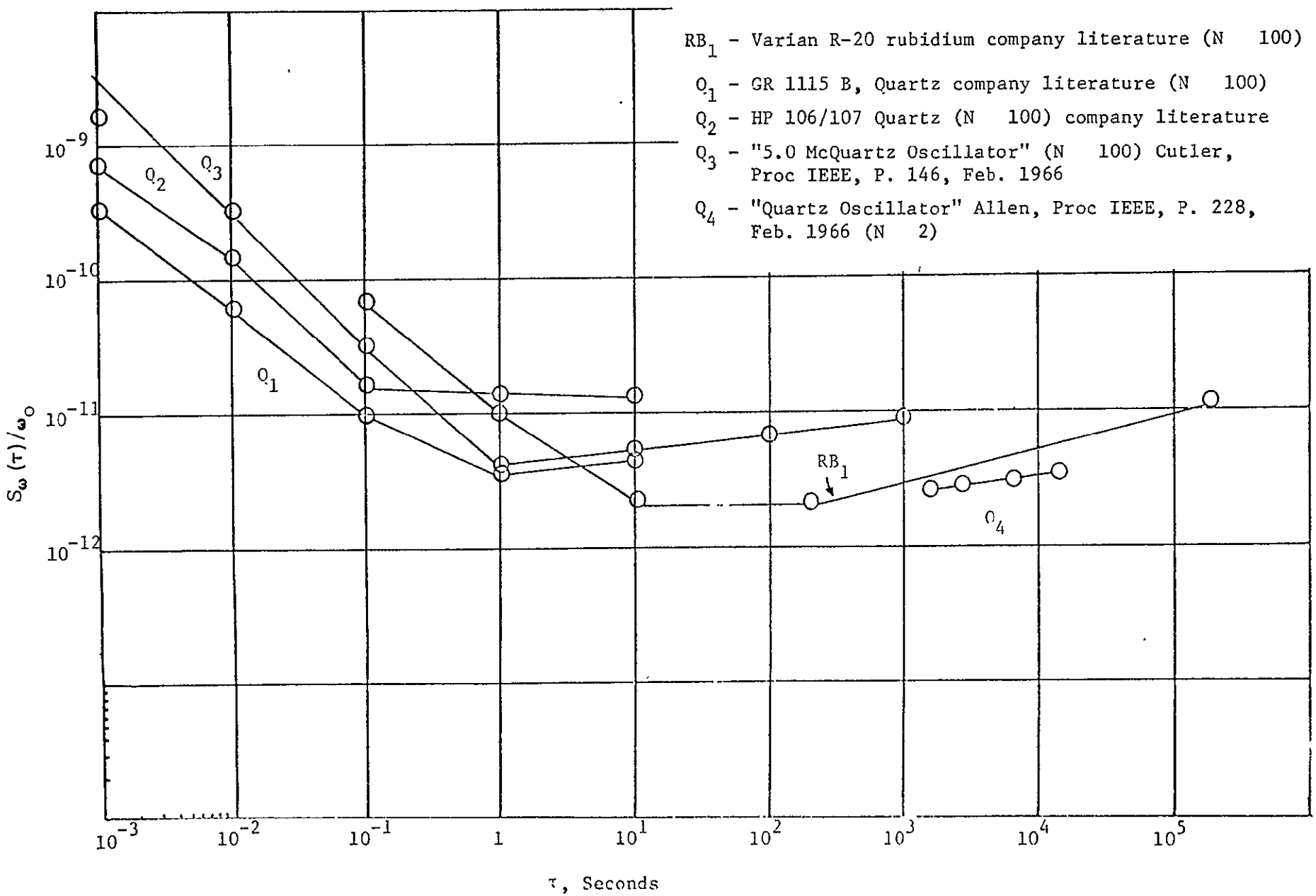

Figure C-1. Actual Oscillator Short Time Stability Functions

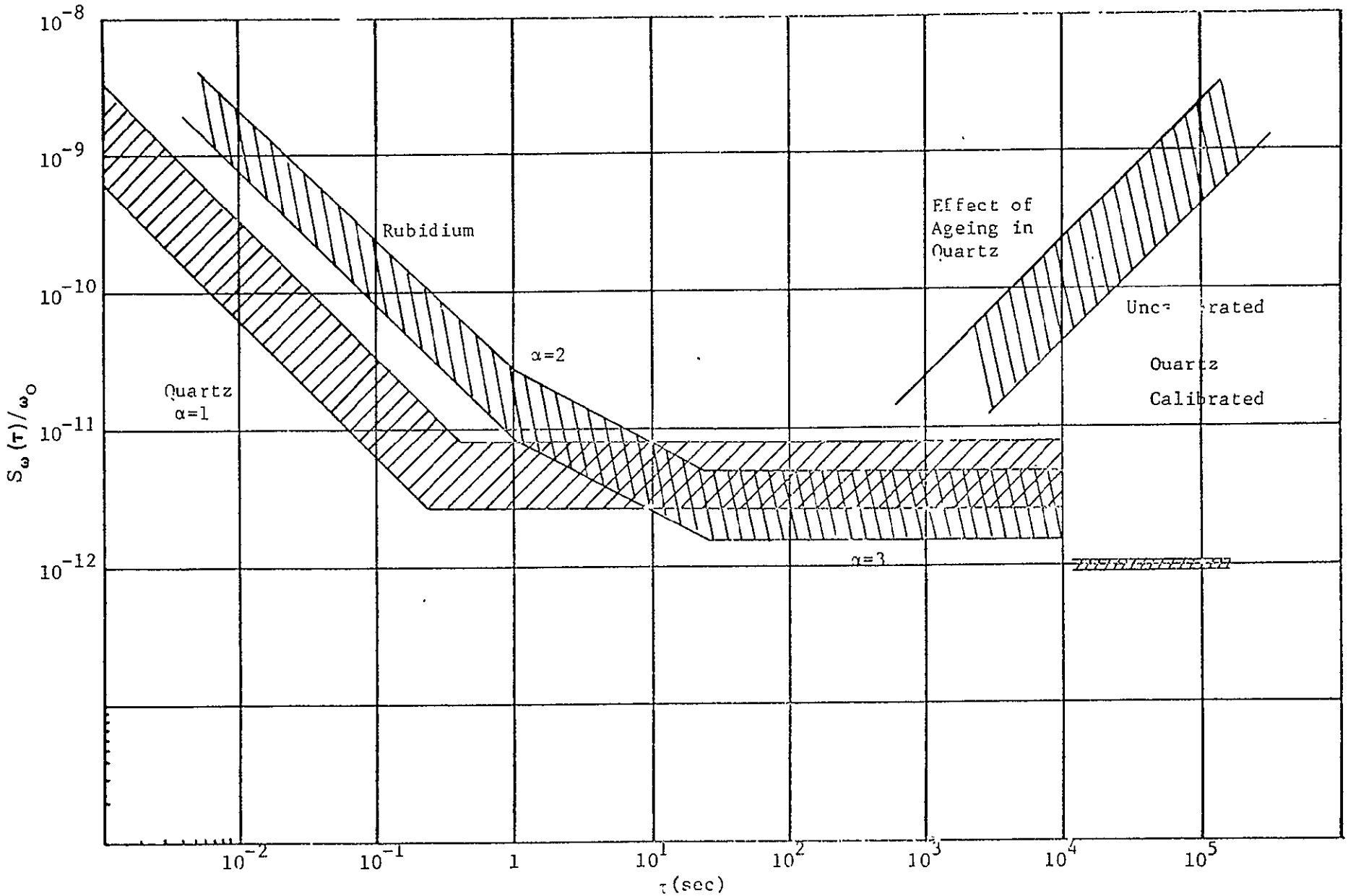

Figure C-2. Idealized Short Time Stability Functions

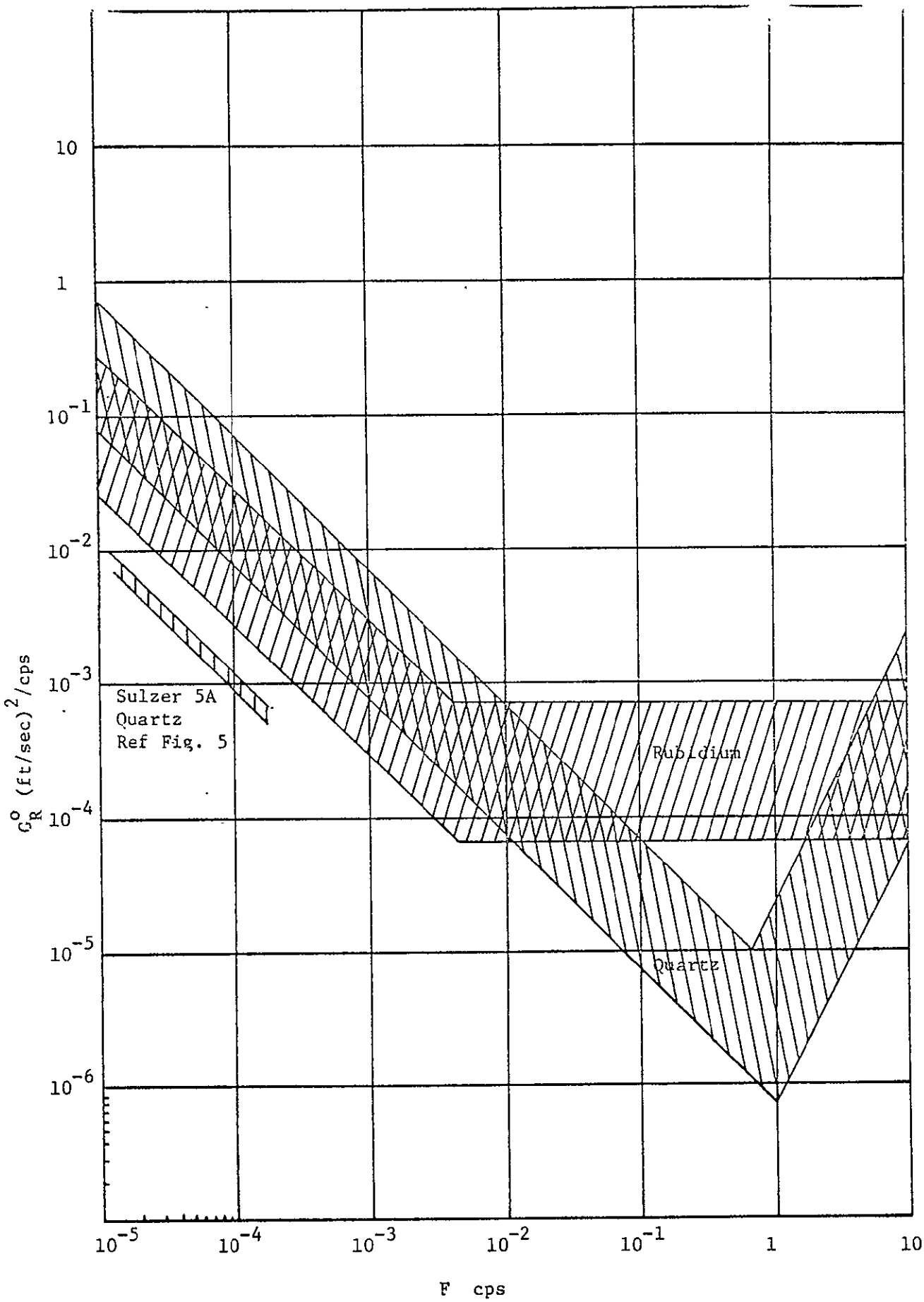

Figure C-3. Velocity Error Spectra Due to Reference Oscillator Error

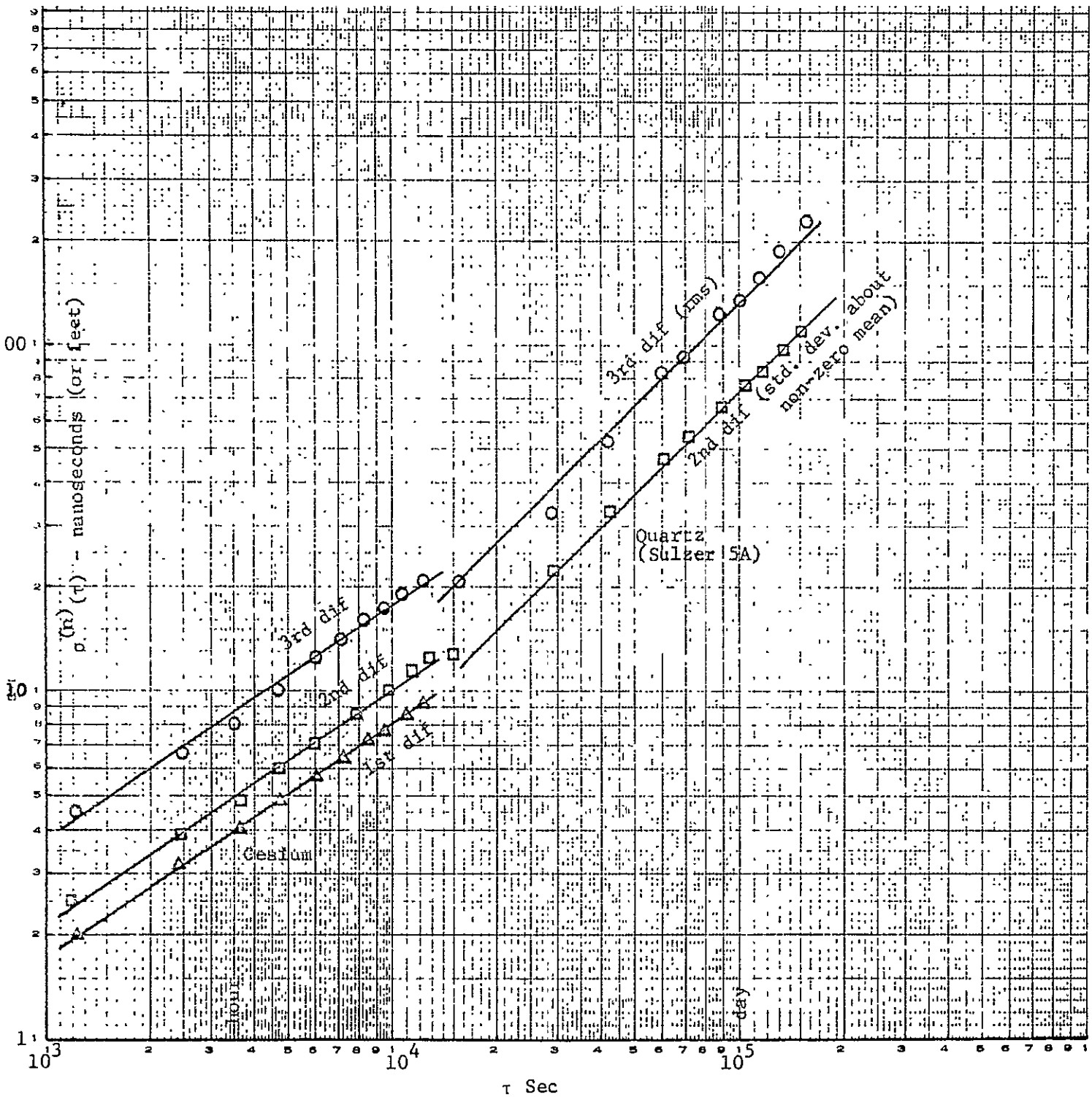

Figure C-4. Barnes' Variate Difference Data

1) This is a Sulzer 5A oscillator which according to Barnes at NBS is the best they have ever found.

2) It has been suggested that as a favored customer NBS may well get the cream of the Sulzer production crop.

3) Constant aging rate effects do not effect the variate difference data whereas, depending on the method of removal of the trend (unspecified), they may or may not enter the short term stability data in Figure C-1 on which the generic characterization is based.

In verbal conversation with Barnes at NBS it was indicated that the best rubidium oscillators show variate differences very similar to those of quartz for times of the order of an hour or more, better by a factor of perhaps 2, while below $\tau = 1$ hour the quartz oscillator is definitely superior.

Direct Interpretation of the Variate Differences

There is an important direct interpretation of the variate differences as given on Figure C-4. Suppose that one performs the following experiment.

1) Measure n values of oscillator phase, or let us say clock time error T, at times

$$t = 0, -\tau, -2\tau, \ldots -(n-1)\tau$$

2) Fit a polynomial of degree $(n-1)$ to those n points.

3) Use the polynomial to extrapolate or predict the time error at a time τ, one step in the future

Note that this is quite closely parallel to the problem of calibrating the satellite oscillator. The fitting and extrapolation problem can be conveniently expressed in terms of the LaGrange interpolation coefficients, thus the extrapolation for the value at 0 in terms of the values at $-\tau$, $-2\tau, \ldots -n\tau$ is given by (Ref. 4, Section 25.2)

$$\hat{T}(0) = \sum_{K=1}^{n} A_K^n \, T(-K\tau)$$

where

$$A_K^n = -(-1)^K \binom{n}{K} \quad K = 1, \ldots n$$

Then the error in extrapolation is

$$\Delta T = \hat{T}(0) - T(0)$$

But, extending the definition of A_K^n to include the case $K = 0$ for which $A_o^n = -1$ we can write

$$\Delta T = \sum_{K=0}^{n} A_K^n \, T(-K\tau)$$

But this is also exactly the concise formula for the nth difference of the T data including the 0th point. (Ref. 4, Section 25.1) Thus, the rms error in extrapolating one τ unit forward based on n equally (τ) spaced points prior is exactly equal to the rms nth difference of the data at interval τ and vice versa.

Thus, for example, we can read Figure C-4 as saying that for a good crystal oscillator, and under equivalent environmental conditions, based on a two-day prior (n = 3 point) calibration, we can extrapolate time for one day forward with an rms error of 130 nanoseconds or 130 feet. The second difference (n = 2) data cannot be interpreted in this way because this represents not the total rms but the standard deviation about a significantly non-zero mean, to determine which requires one additional point in calibration.

The reason for these results being so much better than previously assumed (conservatively as was then pointed out) is because of the effect of aging rate or polynomial component calibration which is not normally taken into account but is taken into account exactly in the variate difference method.

Simulation

The important conclusions regarding simulation are summarized in Figure C-3 which gives the equivalent range rate spectrum due to oscillator frequency error. The frequency range of interest extends roughly from the reciprocal sampling time, to the reciprocal data estimation time, possibly 10^{-2} to 10^{-6} Hz. Over this range the quartz error spectrum is very nearly 1/f in range rate, while the rubidium spectrum is white (f^{o}) at the higher frequencies going into 1/f (note this is power) between about 10^{-3} to 10^{-5} Hz. The white part of this spectrum is easily simulated by known methods but no way of simulating 1/f noise in a finite state model is presently known.

References

1. Mallinckrodt, A.J., "Frequency Synchronization for Doppler Tracking Systems," Part I: Stable Oscillators, CRL 498, 20 April 1965; Part II: Propagation Modes, CRL 509, February 1966.

2. Allan, D.W., "Statistics of Atomic Frequency Standards," Proc. IEEE, Vol. 54, No. 2, p. 221, February 1966.

3. Barnes, J.A., "Atomic Timekeeping and the Statistics of Precision Signal Aeverators," Proc. IEEE, Vol. 54, No. 2, p. 207, February 1966.

4. "Handbook of Mathematical Functions," AMS 55, National Bureau of Standards, U.S. Government Printing Office.

5. McCoubrey, A.O., " A Survey of Atomic Frequency Standards," Proc. IEEE, Vol. 54, No. 2, p. 116, February 1966.

6. "Study of Navigation and Traffic Control Employing Satellites," Proposal No. 8710.000 to NASA-ERC, TRW Systems, January 24, 1967.